

AD-A152 811

CHAIN DYNAMICS AND STRUCTURE PROPERTY RELATION IN HIGH
IMPACT STRENGTH PO. (U) COLLEGE OF THE HOLY CROSS
WORCESTER MA P T INGLEFIELD ET AL. 84 JAN 85

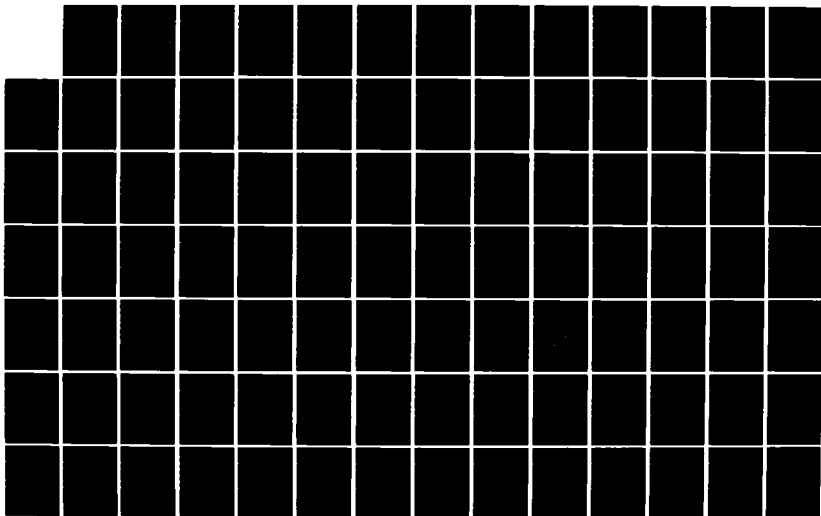
1A

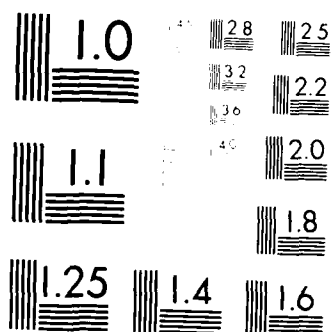
UNCLASSIFIED

ARO-18501. 7-CH-H DARG29-82-G-0001

F/G 11/9

NL





MICROCOPY RESOLUTION TEST CHART
 NATIONAL BUREAU OF STANDARDS-1963-A

2

UNCLASSIFIED

SECURITY CLASSIFICATION OF THIS PAGE (When Data Entered)

REPORT DOCUMENTATION PAGE		READ INSTRUCTIONS BEFORE COMPLETING FORM
1. REPORT NUMBER ARO 18501.7-CH-H	2. GOVT ACCESSION NO. N/A	3. RECIPIENT'S CATALOG NUMBER N/A
4. TITLE (and Subtitle) CHAIN DYNAMICS AND STRUCTURE PROPERTY RELATION IN HIGH IMPACT STRENGTH POLYCARBONATE ELASTIC		5. TYPE OF REPORT & PERIOD COVERED 15 Nov 81 - 14 Nov 84 Final Report
AUTHOR(s) Paul T. Inglefield, Alan A. Jones		6. PERFORMING ORG. REPORT NUMBER
PERFORMING ORGANIZATION NAME AND ADDRESS College of the Holy Cross Worcester, MA 01610		8. CONTRACT OR GRANT NUMBER(s) DAAG29-82-G-0001
CONTROLLING OFFICE NAME AND ADDRESS U. S. Army Research Office Post Office Box 12211 Research Triangle Park, NC 27709		10. PROGRAM ELEMENT, PROJECT, TASK AREA & WORK UNIT NUMBERS
MONITORING AGENCY NAME & ADDRESS (if different from Controlling Office)		12. REPORT DATE January 1985
		13. NUMBER OF PAGES
		15. SECURITY CLASS. (of this report) Unclassified
		15a. DECLASSIFICATION DOWNGRADING SCHEDULE
16. DISTRIBUTION STATEMENT (of this Report) Approved for public release; distribution unlimited.		
17. DISTRIBUTION STATEMENT (of the abstract entered in Block 20, if different from Report) NA		
18. SUPPLEMENTARY NOTES The view, opinions, and/or findings contained in this report are those of the author(s) and should not be construed as an official Department of the Army position, policy, or decision, unless so designated by other documentation.		
19. KEY WORDS (Continue on reverse side if necessary and identify by block number) Polycarbonates Plastics Impact Strength Polymers Molecular Structure Glassy Polymers.		
20. ABSTRACT (Continue on reverse side if necessary and identify by block number) A study of chain dynamics in the solid state of the high impact resistant polycarbonate of bisphenol-A and structural analogues is carried out using nuclear magnetic resonance methods. The object is to quantitatively characterize both the structural geometry and the energetics of local motions occurring in these		

DTIC
SELECTE
MAR 23 1985

B

AD-A152 011

DTIC FILE COPY

Unclassified

SECURITY CLASSIFICATION OF THIS PAGE(When Data Entered)

20. ABSTRACT CONTINUED:

glassy polymers. It is the belief that only through a detailed knowledge of the solid state dynamics can one establish the structural origin of the bulk properties of these materials. It is important that such a study yield a direct connection to the dynamical mechanical properties which form the basis for characterization of high impact materials. One of the first quantitative demonstrations of this connection is noted in this study.

The selection of NMR to probe structure and dynamics in the solid state is well established and the present study focuses on both lineshape and relaxation time analysis using both carbon-13 and deuterium as probes. The study clearly reveals the strengths and weaknesses of the various NMR approaches.



SEARCHED	INDEXED
SERIALIZED	FILED
✓	
PER CALL JC	
A-1	

Unclassified

SECURITY CLASSIFICATION OF THIS PAGE(When Data Entered)

CHAIN DYNAMICS AND STRUCTURE PROPERTY RELATION IN
HIGH IMPACT STRENGTH POLYCARBONATE PLASTIC

FINAL REPORT

Paul T. Inglefield and Alan A. Jones

January 4, 1985

U.S. ARMY RESEARCH OFFICE

GRANT NUMBER DAAG 29-82-G-0001

College of the Holy Cross

Worcester, Mass. 01610

Approved for Public Release;

Distribution Unlimited

The view, opinions and/or findings contained in this report are those of the authors and should not be construed as an official Department of the Army position, policy, or decision, unless so designated by other documentation.

Table of Contents

1. Statement of the problem
2. Summary of most important results
3. List of publications
4. List of scientific personnel
5. Appendix: Compilation of publications

(1) STATEMENT OF THE PROBLEM

A study of chain dynamics in the solid state of the high impact resistant polycarbonate of bisphenol-A and structural analogues is carried out using nuclear magnetic resonance methods. The object is to quantitatively characterize both the structural geometry and the energetics of local motions occurring in these glassy polymers. It is the belief that only through a detailed knowledge of the solid state dynamics can one establish the structural origin of the bulk properties of these materials. It is important that such a study yield a direct connection to the dynamical mechanical properties which form the basis for characterization of high impact materials. One of the first quantitative demonstrations of this connection is noted in this study.

The selection of NMR to probe structure and dynamics in the solid state is well established and the present study focuses on both lineshape and relaxation time analysis using both carbon-13 and deuterium as probes. The study clearly reveals the strengths and weaknesses of the various NMR approaches. It is demonstrated that an extensive data base is desirable in order to provide convincing conclusions. It is important that the structural geometry of the motions be inferred directly and lineshape collapse has this capability. It is also essential that a range of measurements selectively sensitive to different dynamical rates be used. A combination of lineshape collapse and relaxation times (T_1 and $T_{1\rho}$) offers a motional probe from 10^3 to 10^8 sec⁻¹. Further, the use of isotopic labelling of specific backbone sites on the polymer is shown to greatly facilitate analysis in cases where the dynamics is a combination of more than one motional process. The utility of relaxation studies of polymer dynamics in solution on the same or similar molecular systems can be evaluated.

It was also a goal of this study to relate the specific motions observed by NMR to more traditional relaxation experiments on polymers such as dielectric and mechanical response. An interpretation incorporating a wide variety of dynamic information was hoped to provide insight into the ultimate bulk property of impact resistance.

(2) SUMMARY OF MOST IMPORTANT RESULTS

The major thrust of the work has been a detailed characterization of the local chain dynamics in the polycarbonate of bisphenol-A. This has been accomplished with the determination of both the structural details of the motion, the nature of the energetics and the relationship of the motions to the general dynamic properties which characterize the material.

Carbon-13 chemical shift anisotropy (CSA) lineshape analysis on ^{13}C enriched BPA polycarbonates has definitively characterized the geometry of the phenylene group motion as a combination of π flips and restricted rotation. The π flip rate is found to lie on a relaxation map containing the T_1 and $T_{1\rho}$ minima, dielectric loss maxima and dynamic mechanical loss maxima. This broad sampling of dynamics (over eight decades in rate) yields a very convincing quantitative picture. Certain conclusions are immediately apparent:

1. Activation energies obtained assuming a single exponential correlation function and measurements over a limited rate range are inaccurate and generally low.

2. Activation parameters derived using a relaxation map and a non-exponential correlation function approach yield more realistic values for motion in the solid state.

3. A fractional exponential correlation function quantitatively incorporates all of the data including dielectric and mechanical relaxation. This implies a complex or heterogeneous rate and a common underlying dynamic process responsible for all the relaxation phenomena.

A structural model has been proposed to account for all the observed relaxation phenomena and to provide a connection to the observation of high impact resistance. It consists of a cis/trans to trans/trans carbonate conformational interchange leading to a correlated backbone motion which is coupled to the local phenylene π flip. This motion is diffusional in character thus providing a mechanism for the rapid release of stress over macroscopic distances. The fractional exponent ($\alpha = .18$) used in the correlation function quantifies the

complex character of the rate process and indicates motional timescales extending over five decades. This type of behavior is undoubtedly common for solid state kinetics in macromolecular systems. It can be interpreted as arising from a distribution of rates throughout the material (the inhomogeneous case) or from an inherent nonexponential character in a single rate process, possibly arising from the cooperative nature of the dynamics (the homogeneous case).

A model has also been devised (The Simultaneous Model) for the treatment of multi-site exchange processes involving the collapse of solid NMR lineshapes. The method is applicable to both CSA and Quadrupolar lineshape collapse, and is easily computerized for cases involving more than one kinetic process simultaneously contributing to line narrowing. The model introduces a distributional character to conformational interchanges which is physically desirable.

In addition, polycarbonate and polyformal polymer in solution have been investigated using both ^{13}C and ^2H as NMR probes, the detailed local chain dynamics can again be characterized using correlation function approaches based on models for both segmental and local conformational events. The results can be compared with the information obtained from solid state analysis and activation energies compare favorably with those obtained from the fractional correlation function analysis for the microscopic intramolecular process in the absence of coupling to the glass. In many instances it is clear that knowledge previously derived from dynamic studies in dissolved polymers forms a basis for the simulations used to analyze the solid state spectra.

The full details of these remarks are contained in the appendix which is a compilation of the publications resulting from the project.

(3) LIST OF PUBLICATIONS

1. "Solid State NMR Line Shape Analysis of Motion in Glassy Polymers"
P. T. Inglefield, R. M. Amici, A. A. Jones and J. F. O'Gara,
Polymer Preprints 24 (2), 143 (1983).
2. "Solid State Carbon and Proton Line Shapes for the Characterization of
Phenylene Group Motion in Polycarbonates" P. T. Inglefield, R. M. Amici,
J. F. O'Gara, C.-C. Hung and A. A. Jones, Macromolecules 16, 1552 (1983).
3. "Spin Relaxation and Local Motion in a Dissolved Aromatic Poly(ortho)"
M. F. Tarpey, Y.-Y. Lin, A. A. Jones and P. T. Inglefield. Preprints
Division Org. Coating Plastics Chemistry 48, 97 (1983).
4. "Spin Relaxation and Local Motion in a Dissolved Aromatic Poly(ortho)"
M. F. Tarpey, Y.-Y. Lin, A. A. Jones and P. T. Inglefield, NMR and
Macromolecules, ACS Monograph 247, 67 (1984).
5. "Temperature Dependence of Phenyl Group Motion in BPA from Solid State
Carbon-13 Line Shapes" A. A. Jones, J. F. O'Gara and P. T. Inglefield,
Polymer Preprints 25 (1) 345 (1984).
6. "A Molecular Level Model For Motion and Relaxation in Glassy Polycarbonate"
A. A. Jones, Macromolecules, accepted, to appear (1985).
7. "Spin Relaxation and Solution Dynamics of Bisphenol-A Polycarbonate by
Deuterium NMR" J. A. Porco, P. T. Inglefield, J. Campbell and A. A. Jones,
Polymer Preprints, accepted, to appear (1985).
8. "The Temperature Dependence of Local Motions in Glassy Polycarbonate
from Carbon and Proton NMR" J. F. O'Gara, A. A. Jones, C.-C. Hung and
P. T. Inglefield, Macromolecules, accepted, to appear (1985).
9. "A Nuclear Magnetic Resonance Study of the Molecular Dynamics of Various
Polycarbonates" J. F. O'Gara, PhD Thesis, Clark University (1984)
10. "Polymer Motion in the Solid State" A. A. Jones, in "High Resolution NMR
of Synthetic Polymers in Bulk", Verlag Chemie International, R. A. Kom
ed., to appear (1985).
11. "The Application of a Simultaneous Model for Multi-Site Exchange to Solid
State NMR Line Shapes" A. K. Roy, A. A. Jones and P. T. Inglefield, J Mag.
Res., in preparation.

(4) LIST OF SCIENTIFIC PERSONNEL

1. Dr. Paul T. Inglefield (Principal Investigator)
Research Associate and Director, Worcester Consortium NMR Facility
Department of Chemistry
College of the Holy Cross
Worcester, MA 01610
2. Dr. Alan A. Jones (Co-Principal Investigator)
Professor
Department of Chemistry
Clark University
950 Main Street
Worcester, MA 01610
3. John F. O'Gara (Research Assistant)
Department of Chemistry, Graduate Student
Clark University
PhD Clark University June, 1984.
4. The following participated as research assistants to a lesser extent while supported from other sources.

College of the Holy Cross	Robert M. Amici
	John A. Porco
Clark University	C.-C. Hung
	M. F. Tarpey
	A. K. Roy

(5) APPENDIX: COMPILATION OF PUBLICATIONS.

THE FUTURE OF THE FUTURE

A.A. Jones and G.L. Fisher
Jeppson Laboratory, Dept. of Chemistry
Clark University, Worcester, MA 01601

Inter-Action

The line shapes obtained from our own, earlier, and literature NMR studies have been used to characterize the geometry of rotations of lipid polymers. In earlier work, immediately following the introduction of the model, most attention was focused on the motion of the phenylene group and in the first report of group line shape data relevant to phenylene group rotation (1) attention was focused on rotation of restricted rotation about the ω_2 axis is the largest amplitude, highest frequency phenylene group rotation. However, the proton data are completely insensitive to the amplitude of the rotation and whether it proceeds by small steps or large amplitude flips.

Variable temperature carbon-13 magic angle sample spinning spectra of a related p-dimer (13) are also unable to define the latter as a set of the phenylene group motion from a narrow model of the motion of ellips about the C-C axis. Better line shapes are considerably more sensitive to the nature of the motion and, therefore, indicate that the rotation of a plate primarily is ellips about the C-C axis. Carbon-13 spin density rotational spin echo line shape experiments have indicated that it also be explained by a motion of intermediate rotational frequency faster than the spin-lattice relaxation rate of the C-13 nucleus. A significant difference is observed in the chemical shift anisotropy tensor for the two motions and is allowed. Therefore, it appears that the presence of ellips for some motion, means in this system is originally restricted to plates as used in polymer films.

In this report, we present an analysis of the chemical shift anisotropy (A) line shape of a magnetization precession mode in the low temperature limit at -10^3 and in the high temperature limit which persists over a range of about 100 Gauss below it. This analysis is similar with the "broadened precession line" studies reported in the same publication, all ways to more specific conclusions concerning the geometry and magnitude of the motion in bilayers of $\text{Al}(\text{Al})$ polymers.

References

The sample of hydrogenated polybutene, single side, was prepared by the method of the literature and was synthesized from the mixed stream 2-1. The material was 95% 1, 2-polybutene and contained 1% of the hydrogenated polybutene used in the production. Polar line shape measurements were obtained by standard methods, measured in the percent deuteration determined from proton and deuterium spectra of the deuterated polymers. The α and β peaks were obtained using cross polarization and the power is varied method, and the identification of the peaks was obtained from an external reference and a peak at 11.1 ppm. All NMR measurements were done on a Bruker AM-200 200 MHz spectrometer.

2. *Chlorophyll a* and *Chlorophyll b* were determined by the method of Arar and Collins (1971).

[illegible][illegible]

Because the λ_{max} varies with only different shape from real dipolar radiation, this indicates the observed high temperature limit is not too far from the general shape of the lines are composed with fairly large amplitude modulation, and that the decrease in the observed high temperature limit is quite well simulated. Certain other processes also change the high temperature limit. For instance, both the lines between 2 degrees and 4.5 degrees, and rotation about an axis inclined at 30 degrees produce reasonable modifications of the observed spectrum. The maximum of the λ_{max} line above in the observed rotation spectrum is displaced slightly from the observed peak but its shape can be definitively ruled out by considering the precise dipolar line shape.

[illegible]

A line where simultaneous (nearly) rotation about an axis in line with \vec{B} occurs from the \vec{C} axis. This motion would collapse the line splitting in the proton spectrum by 5.

The 11A line share itself ruled out restricted rotation about the C-C bond, but two remaining possibilities consistent with the current neutron data are - first, plus restricted rotation and, - second, free. The first notion seems practically plausible, but while the second is unexpected, it is not unreasonable. In any case, these line share interpretations are in excellent agreement with the presence of - 11A - as determined by studies of a considerable restricted rotation in the crystal.

1. *Phragmites australis* (Cav.) Trin. ex Steud.

- [illegible]

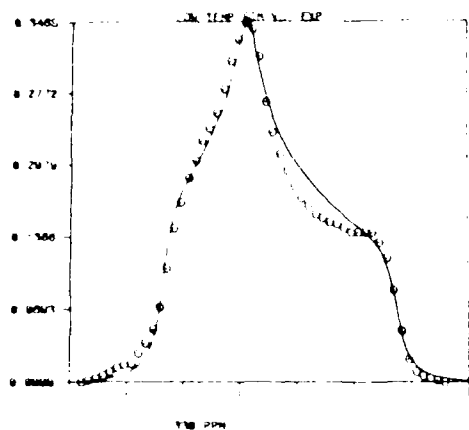


Figure 1. The chemical shift anisotropy line shape in the low temperature limit. The points are experimental data at -120° and the line is the best simulation using the functional form for an axially symmetric chemical shift tensor (9).

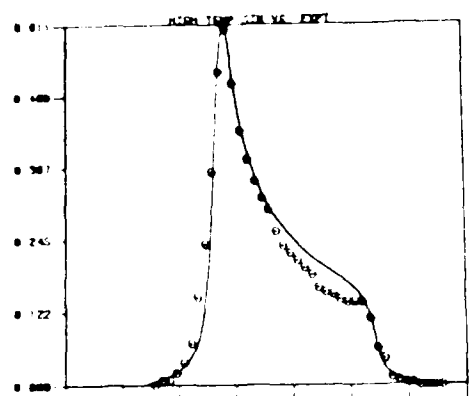


Figure 2. The chemical shift anisotropy line shape in the high temperature limit. The points are experimental data at $+110^\circ$ and the line is the best simulation using the functional form for an axially symmetric chemical shift tensor (9).

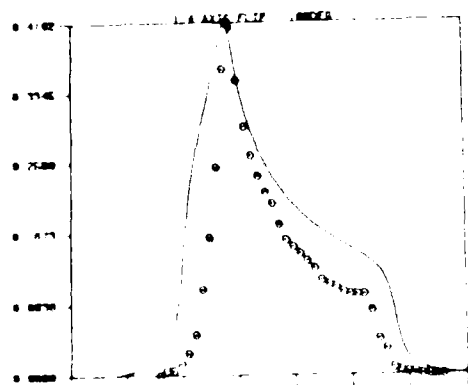


Figure 3. The same as Figure 2, only here the line is the shape resulting from rotational diffusion restricted to a range of 90° in the high temperature limit (11).

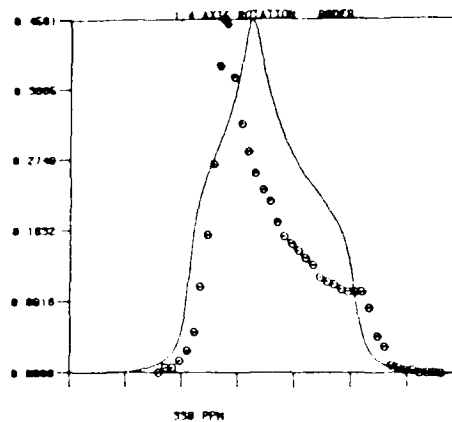


Figure 4. The same as Figure 2, only here the line is the shape resulting from rotational diffusion restricted to a range of 90° in the high temperature limit (11).

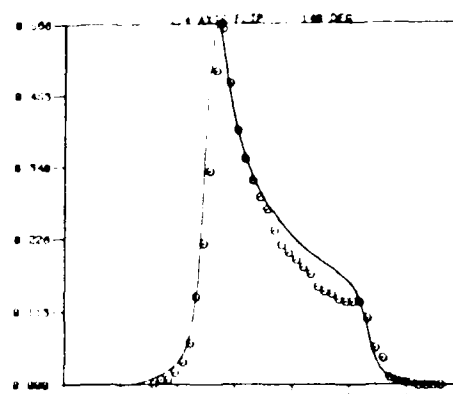


Figure 5. The same as Figure 2, only here the line is the shape resulting from flips between 0 and 140° about the C_2C_3 axis in the high temperature limit (7).

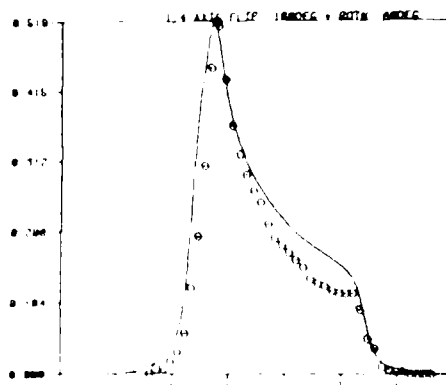


Figure 6. The same as Figure 2, only here the line is the shape resulting from flips about the C_2C_3 axis and rotational diffusion is restricted to a range of 140° about this axis in the high temperature limit (7).

described in two ways. The first description is derived from the action of a three bond jump on a tetrahedral lattice (7) and the second is developed from consideration of computer simulations of backbone transitions in polyethylene chains (8). Anisotropic rotation can also be characterized in several ways. It can be described as jumps between two minima (11), jumps between three minima (12) or stochastic diffusion (12).

In the three bond jump model for segmental motion there are two parameters. The time scale is set by the harmonic average correlation time, τ_h and the effective distribution of correlation times is set by the number of coupled bonds m . The sharp cut off of coupling solution of the three bond jump model is employed here. The composite spectral density for internal rotation by jumps or stochastic diffusion plus segmental motion by three bond jump is

$$J_1(\omega) = \sum_{k=1}^s \frac{2J_k}{1 + \tau_k^{-1} \omega^2} + \frac{B \tau_{hk}^{-1}}{1 + \tau_{hk}^{-1} \omega^2} + \frac{C \tau_{ik}^{-1}}{1 + \tau_{ik}^{-1} \omega^2}$$

$$\tau_{k0}^{-1} = \tau_k^{-1}$$

$$\tau_k = W \tau_k \quad s = (m + 1)/2$$

$$\tau_k = 4 \sin^2[(2k - 1)\pi / 2(m + 1)]$$

$$\tau_h^{-1} = 2W$$

$$s = 1$$

$$G_k = 1/s + (2/s) \exp(-iq) \cos [(2k - 1)\pi q / 2s] \quad (2)$$

$$q = 1$$

$$r = \ln 9$$

$$A = (3 \cos^2 \alpha - 1)/4$$

$$B = 3(\sin^2 \alpha)/4$$

$$C = 3(\sin^4 \alpha)/4$$

for stochastic diffusion

$$\tau_{hk0}^{-1} = \tau_k^{-1} + \tau_{ir}^{-1}$$

$$\tau_{ik0}^{-1} = \tau_k^{-1} + (\tau_{ir}/4)^{-1}$$

for a three bond jump

$$\tau_{hk0}^{-1} = \tau_{k0}^{-1} + \tau_k^{-1} + \tau_{ir}^{-1}$$

Table I. Spin-Lattice Relaxation Times (ms)

^{13}C	Phenyl Protons		Protonated Phenyl Carbons		Formal Protons		Formal Carbons	
	90 MHz	40 MHz	62.9 MHz	22.6 MHz	25.0 MHz	90 MHz	62.9 MHz	22.6 MHz
17	548	153	137	72	335	129	81	46
27	499	189	174	106	282	114	91	52
33	522	274	243	136	263	135	115	67
61	628	432	377	349	295	197	135	123
81	794	553	543	448	350	258	129	193
116	1168	763	798	679	467	320	339	277
127	1411	939	1113	936	628	433	473	377

in the form of nonlinear behavior when the return of the magnetization was plotted in the standard form $\ln(A_\infty - A_t)$ versus t . The presence of cross-relaxation in the proton data was further checked by comparing the phenyl proton T_1 in the partially deuterated analogue with the phenyl T_1 in the fully protonated polymer. The phenyl proton T_1 is about 10% longer in the deuterated polymer indicating a small amount of cross-relaxation though the 10% change is essentially the same as the experimental uncertainty. A 10% uncertainty is placed on all T_1 values, reflecting error contributions from concentration, temperature and pulse widths as well as random fluctuations in intensity. Table I contains proton and carbon-13 T_1 's as a function of temperature and Larmor frequency.

Interpretation

The standard relationships between T_1 's and spectral densities J 's are employed. For carbon-13, the expressions are (4)

$$1/T_1 = W_0 + 2W_{1C} + W_2$$

$$W_0 = \sum_j \gamma_C^2 \gamma_H^2 h^2 J_1(\omega_0) / 20 r_j^6 \quad (1a)$$

$$W_{1C} = \sum_j \gamma_C^2 \gamma_H^2 h^2 J_1(\omega_C) / 40 r_j^6$$

$$W_2 = \sum_j \gamma_C^2 \gamma_H^2 h^2 J_2(\omega_2) / 10 r_j^6$$

$$\omega_0 = \omega_H - \omega_C \quad \omega_2 = \omega_H + \omega_C$$

and for protons it is

$$1/T_1 = \sum_j \gamma^4 h^2 r_j^{-6} \{ (2/15) J_1(\omega_H) + (8/15) J_2(2\omega_H) \} \quad (1b)$$

The internuclear distances employed are 1.095 Å for the phenyl C-H distance, 1.125 Å for the formal C-H distance, 2.4 Å for the 2-3 phenyl proton distance, and 1.75 Å for the formal proton - proton distance. The 2-3 phenyl proton distance used here is comparable to the distance of 2.41 Å used in the polycarbonate interpretations. The choice of 2.4 Å is based on the phenyl proton T_1 minimum and the slightly smaller value is confirmed by a larger Pake doublet splitting observed in the solid state spectrum of the phenyl protons in the partially deuterated analogue (10).

Expressions for the spectral density can be developed from models for local motion in randomly coiled chains. Two general types of local motion will be considered, and they are segmental motion and anisotropic rotation. Segmental motion itself will be

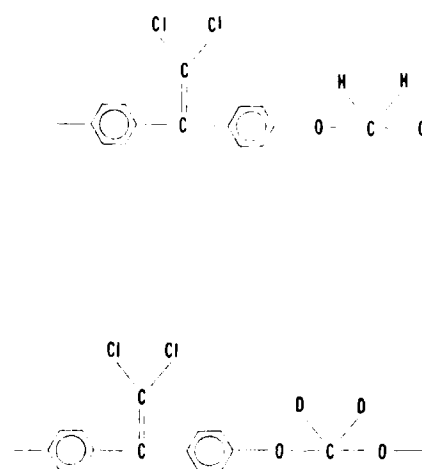


Figure 1. Structure of the polyformal repeat unit and the partially deuterated analogue.

Spin relaxation in dilute solution has been employed to characterize local chain motion in several polymers with aromatic backbone units. The two general types examined so far are polyphenylene oxides (1-2) and aromatic polycarbonates (3-5); and these two types are the most common high impact resistant engineering plastics. The polymer considered in this report is an aromatic polyformal (see Figure 1) where the aromatic unit is identical to that of one of the polycarbonates. This polymer has a similar dynamic mechanical spectrum to the impact resistant polycarbonates (6) and is therefore an interesting system for comparison of chain dynamics.

In addition, the formal unit itself offers a new opportunity for monitoring chain motion relative to the polycarbonates since the carbonate unit contains no protons. The spin-lattice relaxation times, T_1 's of all protons and all carbons with directly bonded protons are reported for the polyformal. Also the carbon and proton T_1 's are measured at two different Larmor frequencies to expand the frequency range covered by the study.

In addition to determining the time scales for several local motions in polyformal, two different interpretational models for segmental motion will be employed. An older model by Jones and Stockmayer (7), based on the action of a three bond jump on a tetrahedral lattice is compared with a new model by Weber and Helfand (8), based on computer simulations of polyethylene type chains. These two models for segmental motion have been compared before (5) for two polycarbonates but somewhat different results are seen in the polyformal interpretation.

Experimental

High molecular weight samples of the polyformal were kindly supplied by General Electric. The structure of the repeat unit is shown in Figure 1 as well as the structure of a partially deuterated form which was synthesized (9) to reduce proton cross-relaxation. A 10 weight percent solution of the polymer in deuterated tetrachloroethane was prepared in an NMR tube, subjected to five freeze, pump, thaw cycles and sealed.

Spin lattice relaxation measurements were conducted on two spectrometers with a standard π - τ - $\pi/2$ pulse sequence. The 30 and 90 MHz proton measurements as well as the 22.6 MHz carbon-13 measurements were made on a Bruker SXP 20-100. The 250 MHz proton and 62.9 carbon-13 measurements were made on a Bruker WM-250.

Results

Spin lattice relaxation times are calculated from the return of the magnetization to equilibrium using a linear and non-linear least squares analysis of the data. The two analyses yield T_1 values within 10% of each other and average values are reported. No evidence of cross-relaxation or cross-correlation were observed

Spin Relaxation and Local Motion in a Dissolved Aromatic Polyformal

M. L. FARPLY, Y.-Y. LIN, and ALAN ANTHONY JONES

Jeppson Laboratory, Department of Chemistry, Clark University, Worcester, MA 01610

P. L. INGELHELD

Department of Chemistry, College of the Holy Cross, Worcester, MA 01610

Carbon-13 and proton spin-lattice relaxation times are reported for 10 wt% solutions of a dissolved aromatic polyformal. The relaxation times for both nuclei were determined at two Larmor frequencies and as a function of temperature from 0 to 120°C. These relaxation times are interpreted in terms of segmental motion and anisotropic internal rotation. Segmental correlation functions by both Jones and Stockmayer, and Weber and Helfand were used to interpret the data. Internal rotation is described by the usual Woessner approach, and restricted rotational diffusion, by the Gronski approach. Both segmental correlation functions lead to similar results; but, relative to the analogous polycarbonate, single bond conformational transitions are more frequent in the polyformal. The phenyl groups in the backbone undergo segmental rearrangements and internal anisotropic rotation at comparable rates. Motion in the formal linkage is described by the same segmental correlation times plus restricted rotational diffusion about an axis between the oxygens of the formal group. The interpretation at the formal link based on restricted rotational diffusion is discussed in terms of the conformations likely in the link which are commonly referred to as the anomeric effect. The choice of the axis of restricted rotation in the formal unit is only an approximation of the result of anisotropic single bond conformational transitions occurring within that unit.

Table I: (continued)

T (°C)	Formal Proton T ₁ (ms) exp/sim 1/sim 2(b)		Formal Carbon T ₁ (ms) exp/sim 1/sim 2(b)	
	250 MHz	90 MHz	62.9 MHz	22.6 MHz
0	335/316/217	129/118/102	81/79/77	36/34/40
20	282/278/215	113/133/113	91/93/84	52/54/57
40	255/274/237	133/151/141	101/115/109	82/81/80
60	267/292/276	198/190/183	134/142/143	123/111/115
80	311/345/345	258/235/235	188/181/181	193/147/147
100	356	320	241	328
120	455	433	394	366

(a) The 90 MHz phenyl proton data were taken on a sample in which the formal protons were replaced by deuterons. As of the date of this preprint, 30 MHz data has not been taken on the partially deuterated form.

(b) sim 1 is the simulation allowing for only restricted anisotropic rotational diffusion about the oxygen-oxygen axis. Sim 2 is the simulation allowing for complete anisotropic rotational diffusion about the oxygen-oxygen axis.

Table II: Simulation Parameters for T₁'s in Table I

T (°C)	Seg- mental		Phenyl Group Rotation	Formal Group Rotation		
				sim 1	sim 2	
	τ_h (ns)	π	τ_{irp} (ns)	τ_{irf} (ns) Full Rotation	Angle Per Restricted Rotation	D _{ir} × 10 ⁻¹⁰ (s ⁻¹) Restricted Rotation
0	1.34	3	2.10	1.9	81°	0.082
20	0.70	3	1.53	1.75	110°	0.15
40	0.364	3	1.15	1.30	140°	0.16
60	0.210	3	0.46	1.00	150°	0.16
80	0.106	5	0.44	1.00	360°	0.16
100	0.045	9	0.39			
120	0.030	11	0.35			

Thus in a chain of OCH_2 units, polyoxymethylene, it would not be possible to separate segmental motion from restricted anisotropic rotation in the same way. Even the attempt made here rests on a limited data base and crude models though the data base is fairly extensive by current standards as is the sophistication of the models.

Acknowledgements

The research was carried out with financial support of the National Science Foundation, Grant DMR-790677, of National Science Foundation Equipment Grant No. CHE 77-09059, and of National Science Foundation Grant No. DMR-8108679 and supported in part by the U.S. Army Research Office, Grant #DAA929-82-G-0001.

References

1. R.E. Cais and F.A. Bovey, *Macromolecules* (1977), 10, 752.
2. G.C. Levy, D.E. Axelson, R. Schwartz and J. Hochmann, *J. Am. Chem. Soc.* (1978), 100, 410.
3. F.C. Schilling, R.E. Cais and F.A. Bovey, *Macromolecules* (1978), 11, 325.
4. S. Mashimo, *Macromolecules* (1976), 9, 91.
5. J.F. O'Gara, S.G. Desjardins and A.A. Jones, *Macromolecules* (1981), 14, 64.
6. W. Gronski and N. Murayama, *Makromol. Chem.* (1978), 179, 1521.
7. W. Gronski, *Makromol. Chem.* (1979), 180, 1119.

Table I: Experimental and Simulated T_1 's for the Polyformal as a 10 Weight Percent Solution in $\text{C}_2\text{D}_2\text{Cl}_4$

T (°C)	Phenyl Proton ^(a) T_1 (ms) exp/sim		Phenyl Carbon ^(a) T_1 (ms) exp/sim	
	90 MHz	30 MHz	62.9 MHz	22.6 MHz
0	548/540	153/167	137/132	72/79
20	499/506	189/189	174/160	106/109
40	522/509	274/274	221/206	145/158
60	623/592	432/432	329/350	349/316
80	794/784	553/553	448/445	448/405
100	1168/1102	763/771	633/655	679/612
120	1411/1396	939/949	781/814	727/758

seems trivial since NT_1 for the formal carbon is the same as NT_1 for the protonated phenyl carbon. However the phenyl carbon T_1 's are interpreted both in terms of a segmental motion and a phenyl group rotation. Thus the formal group must enjoy additional motions beyond those characterized as segmental motions based on the phenyl proton relaxation.

Several motions were modelled to try to account for proton and carbon-13 at the formal position. First we assumed that whatever segmental motions occurred at the large phenyl groups also involved the formal group. No physically relevant model was chosen here, but only the position that the segmental motions involving the phenyl groups would also involve the formal group.

To account for the observed T_1 's some additional motion must occur. First anisotropic rotation about the OC bond in the OCH_2O unit was considered but this did not account for the observed data. The second approach was to allow anisotropic rotation or restricted anisotropic rotation about the OO axis in the OCH_2O unit. The restricted rotation accounts for the data from 0° to 60° better than complete rotation although a fairly large angle for restricted diffusion results. At 80° , the best simulation of that is achieved when complete anisotropic rotation about the OO axis is allowed. The Gronski approach⁶⁻⁷ is used to describe restricted rotation though other models could be considered. In Table II, the column labeled sim 1 refers to restricted anisotropic rotation and sim 2 refers to complete anisotropic rotation via stochastic diffusion. Note again, at 80° the optimum angle of restriction is 360° which corresponds to complete anisotropic rotation. The diffusion constant for the restricted case is D_{ir} and the correlation time for the complete rotation case is τ_{irf} .

Above $80^\circ C$, no interpretation of the formal relaxation was pursued since the extreme narrowing limit is nearly achieved. Better measurements over a wider frequency range will be made before this aspect is completed.

Conclusions

The description of motion developed on the basis of the spin relaxation for the phenyl group is similar to the earlier studies of polycarbonates.⁵ Phenyl group rotation is slower in the formal relative to the analogous polycarbonate. This difference in phenyl group rotation is also seen in the solid carbon-13 magic angle sample spinning spectra which show a doublet in the polyformal and a singlet in the polycarbonate for the protonated phenyl carbon at room temperature. No evidence for restricted phenyl group rotation is observed in solution.

The formal group is best interpreted thus far by segmental motion plus anisotropic restricted rotational diffusion about the OO axis of the OCH_2O unit. The angle over which restricted diffusion occurs increases with temperature while the diffusion constant remains relatively constant. The presence of a restricted rotation in a chain backbone is an interesting phenomenon if the data and modelling are to be believed. Without the presence of an internuclear interaction parallel to the chain backbone provided by the phenyl protons, the distinction between segmental motion yielding overall isotropic relaxation and some sort of partial anisotropic rotation could not have been made.

to remove cross relaxation between the phenyl protons and the formal protons. By comparison to the polycarbonates studied earlier, the replacement of the carbonate unit by the formal unit, gives more positions for NMR relaxation study. The additional data gained from the formal protons and formal carbon are the basis for some new insights into chain dynamics.

Experimental Results

High molecular weight polyformal of 1,1-dichloro-2,2 bis(4-hydroxy phenyl)ethylene was used to prepare 10 weight percent solutions of polymer in $C_2D_2Cl_4$. This polymer was kindly supplied by General Electric, Research and Development Center. Carbon-13 spin-lattice relaxation times, T_1 's were measured at 22.6 MHz in a Bruker SXP 20-100 and at 62.9 MHz in a Bruker WM 250. Only values for protonated carbons are reported in Table I, and the two protonated phenyl carbons have the same T_1 which is reported. Proton T_1 's were measured at 30 and 90 MHz in the SXP; and at 250 MHz, in the WM 250. Measurements were made as a function of temperature over the range of 0 to 120°C and all results are included in Table I.

Interpretation

A preliminary scan of the data in Table I shows that from 0 to 30°C, the extreme narrowing limit is not achieved. Above 30°C, the extreme narrowing limit is approximately in effect which results in less information content at the higher temperature. The NT_1 rule is also nearly valid when comparing the phenyl carbon data ($N=1$) with the formal carbon data ($N=2$).

The phenyl proton and carbon-13 data are interpreted in the same manner as reported for the studies of polycarbonates.⁵ The phenyl group is considered to undergo two general types of motion: segmental rearrangements and phenyl group rotation. Segmental motion resulting from changes in the direction of the units composing the backbone is assumed to follow a correlation function of the form developed by considering 3 bond jumps on a tetrahedral lattice with a sharp cutoff of coupling. Phenyl group rotation is described by stochastic diffusion about the C_1C_4 axis.

To characterize segmental motion the phenyl proton data are considered first. In the partially deuterated form, the phenyl protons relax by a dipole-dipole interaction between the 2 and 3 phenyl protons, parallel to the C_1C_4 axis. Therefore, phenyl proton relaxation results only from segmental motion and is unaffected by the presence or absence of phenyl group rotation. Phenyl group rotation can be detected in the phenyl carbon data by checking for a change in relaxation from that predicted by the description of segmental motion developed from the proton data.⁵ In the polyformal, there is evidence for moderately facile phenyl group rotation. Correlation times τ_1 for segmental motion and correlation times for phenyl group rotation τ_{1p} are shown in Table II. However, relative to similar polycarbonates, phenyl group rotation is 2 to 5 times slower.

If motion at the formal group is now considered, some interesting new aspects arise. It should be remembered, that there are no comparable data in the polycarbonates since there are no protons or carbons with directly bonded protons in the carbonate linkage. At first glance, the formal group motion

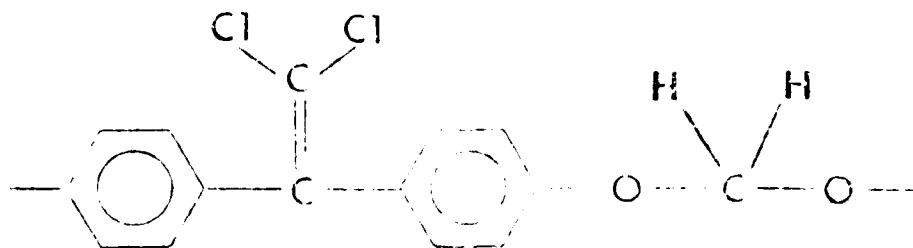
SPIN RELAXATION AND LOCAL MOTION IN A DISSOLVED AROMATIC POLY-FORMAL. M.F. Tarpey, Y.-Y. Lin and A.A. Jones, Jeppson Laboratory, Department of Chemistry, Clark University, Worcester, MA 01610. P.T. Inglefield, Department of Chemistry, College of the Holy Cross, Worcester, MA 01610.

Introduction

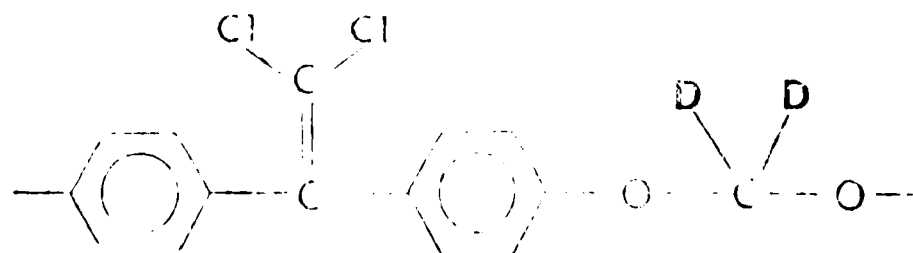
The introduction of commercial instruments for solution carbon-13 NMR over a decade ago spurred many studies of chain dynamics in dissolved macromolecules. The power of NMR as a technique for probing motion lies within its ability to monitor several positions within a repeat unit. This allows for distinguishing several types of local motion based on the repeat unit geometry and the position of the carbon-13 nuclei being probed.¹ The limitation of NMR as a probe of dynamics followed from the restricted frequency range usually studied.²⁻³ Most NMR studies were based on data at one or two frequencies while, for example, dielectric relaxation measurements are made over at least a decade or two of frequency.⁴ In NMR, the lack of dynamic information over a reasonable frequency range has prevented the development of quantitative distinctions between various models for chain motion.

The availability of superconducting spectrometers at ever increasing field strengths offers at least some hope of overcoming the limited frequency range of most NMR studies. These superconducting measurements would have to be combined with low field, conventional magnet measurements;²⁻³ and the simultaneous determination of proton and carbon-13 relaxation also extends the frequency range under consideration.⁵ The addition of proton measurements also increases the number of positions being probed within the repeat unit of the polymer chain.

With the preceding ideas in mind, studies of dissolved polycarbonates have been underway for several years.⁵ Here, the results on an aromatic polyformal, a structural analog of the polycarbonates, is presented. The polymer under consideration is the polyformal of 1,1-dichloro-2,2 bis (4-hydroxy phenyl) ethylene with the repeat unit structure:



To obtain even better proton relaxation data, a partially deuterated analog was prepared:



McMaster, E. W. Byrnes, and J. Campbell for synthesis of the carbon-13 labeled monomer and polymer. The research was carried out with financial support of the U.S. Army Research Office (Grant DAAG 29-82-G-0001) and the National Science Foundation (Grants DMR-790677, CHE 77-09059, and DMR-8108679).

Registry No. Bisphenol A polycarbonate, 24936-68-3; carbonic acid-bisphenol A copolymer, 25037-45-0.

References and Notes

- (1) Inglefield, P. T.; Jones, A. A.; Lubianez, R. P.; O'Gara, J. F. *Macromolecules* **1981**, *14*, 288.
- (2) Schaefer, J.; Sefcik, M. D.; Stejskal, E. O.; McKay, R. A.; Dixon, W. T. "28th Macromolecular Symposium Proceedings"; International Union of Pure and Applied Chemistry, 1982, p. 27.
- (3) Garroway, A. N.; Ritchey, W. M.; Moniz, W. B. "28th Macromolecular Symposium Proceedings"; International Union of Pure and Applied Chemistry, 1982, p. 1.
- (4) Spiess, H. W. "28th Macromolecular Symposium Proceedings"; International Union of Pure and Applied Chemistry, 1982, p. 35. *Colloid Polym. Sci.* **1983**, *261*, 193.
- (5) Garroway, A. N.; Ritchey, W. M.; Moniz, W. B. *Macromolecules* **1982**, *15*, 1051.
- (6) Schaefer, J., private communication.
- (7) Schaefer, J.; Sefcik, M. D.; Stejskal, E. O.; McKay, R. A.; Dixon, W. T.; Carr, R. E. *Prepr. Div. Org. Coat. Plast. Chem.* **1983**, *18*, 87.
- (8) Skottfeldt-Ellingsen, D.; Resing, H. A. *J. Phys. Chem.* **1980**, *84*, 2204.
- (9) Nye, J. F. "The Physical Properties of Crystals", Oxford Press: London, 1967.
- (10) Mehring, M. *NMR Basic Princ. Prog.* **1976**, *11*.
- (11) Jones, A. A.; O'Gara, J. F.; Inglefield, P. T.; Bendler, J. T.; Yee, A. F.; Ngai, K. L. *Macromolecules* **1983**, *16*, 658.

Paul T. Inglefield* and Robert M. Amici

*Department of Chemistry
College of the Holy Cross
Worcester, Massachusetts 01610*

**John F. O'Gara, Chi-Cheng Hung, and
Alan Anthony Jones**

*Jappson Laboratory, Department of Chemistry
Clark University, Worcester, Massachusetts 01610*

Received May 17, 1983

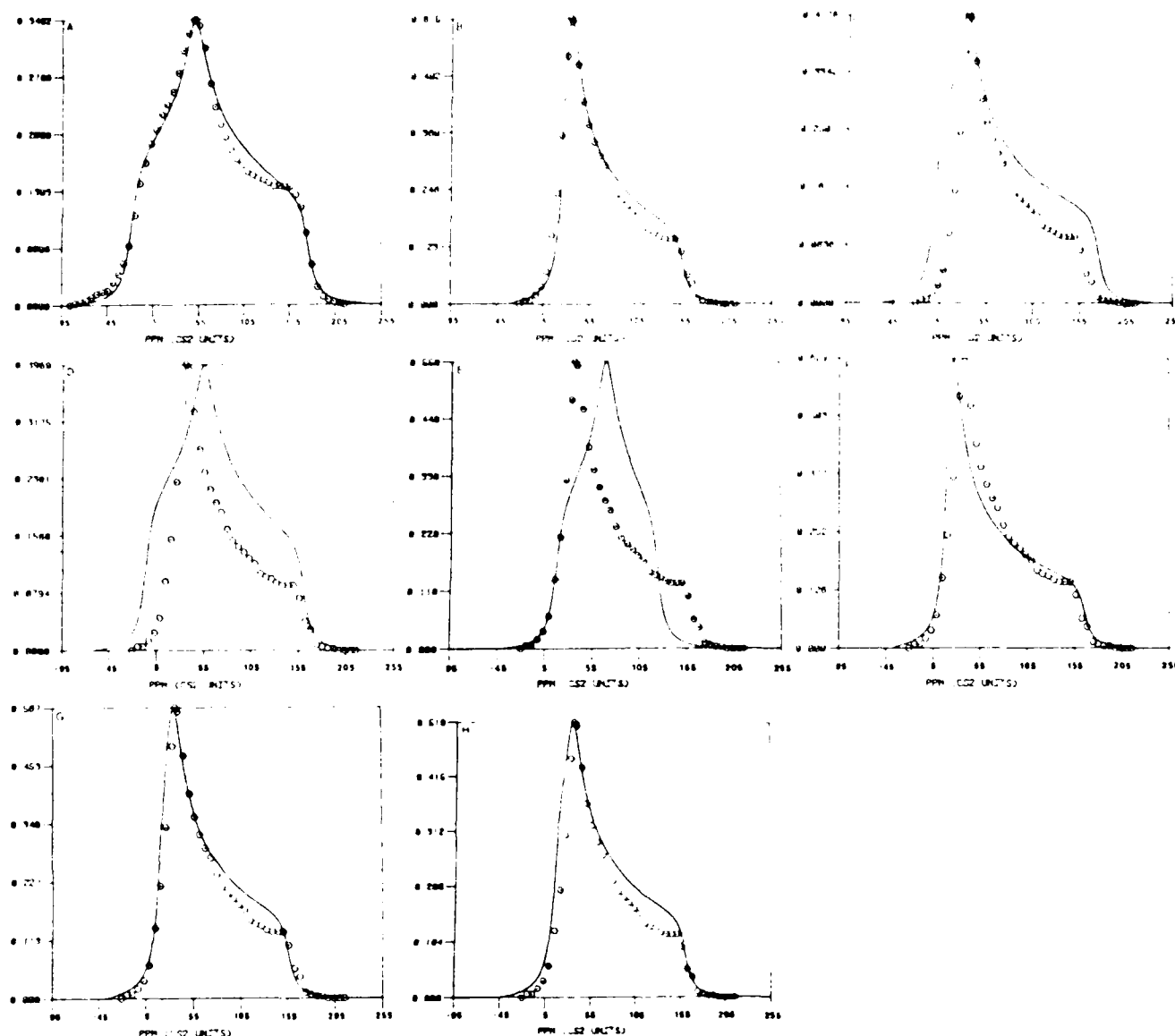


Figure 1. ^{13}C chemical shift anisotropy (CSA) line shapes: (A) low-temperature data and simulation based on powder pattern function;¹⁰ (B) high-temperature data and simulation based on powder pattern function;¹⁰ (C) high-temperature data and simulation based on π flips about the C_1C_4 axis; (D) high-temperature data and simulation based on restricted rotation about the C_1C_4 axis over a 60° range; (E) high-temperature data and simulation based on restricted rotation about the C_1C_4 axis over a 120° range; (F) high-temperature data and simulation based on restricted rotation over a 180° range about an axis inclined at 70° to C_1C_4 (parallel to the $\text{O}-\text{CO}$ bond axis); (G) high-temperature data and simulation based on flips between 0 and 140° about the C_1C_4 axis; (H) high-temperature data and simulation based on C_1C_4 axis π flips plus restricted rotation over a 60° range. The points represent experimental data and the line the theoretical simulations.

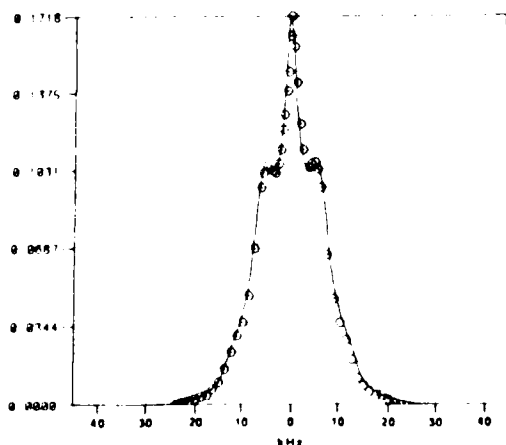


Figure 2. ^1H dipolar line shapes of BPA-d_6 in perdeuterio-BPA. The points represent experimental data and the line the theoretical simulations in the high-temperature limit simulation.

by 70° from the C_1C_4 axis. This motion would collapse the Pake splitting in the proton spectrum by 50% rather than the 10% or less observed.

The CSA line shape itself ruled out restricted rotation about the C_1C_4 axis, but two remaining possibilities consistent with both the carbon and proton data are π flips plus restricted rotation and flips between 0 and 140° . The first motion seems physically plausible; while the second is unexpected, it is not inconceivable. In any case, these line shapes are consistent with the presence of π flips if considerable restricted rotation is also present. This interpretation is in excellent agreement with the model presented by Spiess⁴ based on deuterium line shape measurements. It should be noted that this author suggested that the amplitudes of the restricted rotations are not identical for different phenyl groups, and this could be responsible for the minor discrepancies present in the simulations.

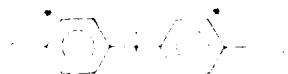
Acknowledgment. We are grateful to Drs. P. D.

Solid-State Carbon and Proton Line Shapes for the Characterization of Phenylene Group Motion in Polycarbonates

The line shapes obtained from proton, carbon, and deuterium magnetic resonance have been used to characterize the geometry of motions in solid polymers, including polycarbonates.¹⁻⁵ In polycarbonates, much attention has focused on the motion of the phenylene group; the first report of proton line shape data relevant to phenylene group motion¹ pointed to some form of rotation or restricted rotation about the C₁C₄ axis as the largest amplitude, highest frequency phenylene group motion. However, the proton data are completely insensitive to the amplitude of the rotation and whether it proceeds by small steps or large-amplitude flips.

Variable-temperature carbon-13 magic angle sample spinning spectra on a related polymer^{2,3} are also unable to define the latter aspects of the phenylene group motion though Garroway et al. modeled the motion as π flips about the C₁C₄ axis. Deuterium line shapes are considerably more sensitive to the nature of the motion, and Spiess⁴ concluded that the rotation took place primarily as π flips about the C₁C₄ axis. Carbon-proton dipolar rotational spin-echo line shape experiments by Schaefer⁵ could also be explained by π flips or alternatively by rotational diffusion restricted to an angular range of about 50°. Schaefer⁶ noted that theoretical simulations in the high-temperature limit of deuterium or dipolar line shapes for π flips are rather similar to certain choices of restricted angular diffusion and therefore difficult to distinguish. On the other hand, a significant difference is predicted in the chemical shift anisotropy tensor for the two motions, and this allowed Schaefer⁷ to substantiate the presence of π flips for some phenyl groups in polystyrene as originally reported by Spiess⁴ based on deuterium data.

In this communication, we report the chemical shift anisotropy (CSA) line shape for a phenyl carbon in polycarbonate in the low-temperature limit at -160 °C and in the high-temperature limit which persists over a range of about 100 °C below T_g . These spectra, shown in Figure 1, were obtained on a carbon-13 labeled polycarbonate of bisphenol A where 90% of one of the two carbons in the phenylene group ortho to the carbonate are isotopically enriched. Either a simple π -2 pulse or cross polarization



followed by proton dipolar decoupling was found to yield adequate CSA spectra below T_g . At low temperatures, the CSA spectrum is distinctly asymmetric, which allows for a more definitive characterization of dynamics than either deuterium or dipolar line shapes, which are essentially axially symmetric. Indeed as shown in Figure 1, the attempts to simulate the high-temperature limit,^{8,9} which is nearly axially symmetric, clearly distinguishes between fairly large-amplitude restricted rotational diffusion and π flips. The simulations utilize the principal values of the shielding tensor observed at low temperatures ($\sigma_{11} = -17$, $\sigma_{22} = 52$, $\sigma_{33} = 175$ ppm on the CS₂ scale) and assumes the orientation of the principal axes reported for benzene.¹⁰ The chemical shift tensor in the principal axis system σ_{112}

can be transformed with the appropriate matrix, **R**, to a desired molecular axis system (σ'_{112}), where the *x* axis is selected as the axis of rotation. $\sigma'_{112} = \mathbf{R}\sigma_{112}\mathbf{R}^{-1}$. Rotation about the *x* axis by an angle α gives $\sigma'_{112}(\alpha) = R_\alpha\sigma'_{112}$. R_α and the CSA line shape corresponding to either flips or restricted rotation about this axis are then generated. Besides π flips having a significantly different shape from restricted rotation, neither replicates the observed high-temperature limit, though π flips are close to the general shape. If π flips are combined with fairly large-amplitude restricted rotation (60°), the observed high-temperature limit is quite well simulated.

Certain other processes also simulate the high-temperature limit. For instance, both flips between 0 and 140° about the C₁C₄ axis and restricted rotation about an axis inclined at 70° produce reasonable replications of the observed spectrum. The maximum of the CSA line shape in the 70° axis rotation spectrum is slightly displaced from the observed peak, but this shape can be definitively ruled out by considering the proton dipolar line shape.

As mentioned, proton dipolar line shapes for the phenylene protons in the polycarbonate of 1,1-dichloro-2,2-bis(4-hydroxyphenyl)ethylene (chloral) have been reported.¹ Since this polymer contains only phenylene protons with one major intramolecular dipole-dipole interaction parallel to the chain backbone, the persistence of this interaction at high temperature implies motions that do not significantly reorient the C₁C₄ axis.¹ The simplest motion meeting this requirement is some form of rotation about that axis though rotations about a parallel axis are also possible candidates.¹¹

To perform the analogous proton dipolar experiment on BPA as just discussed for the chloral polycarbonate, it was necessary to deuterate the methyl groups to produce BPA-*d*₆. A level of 98% deuteration of the methyl groups was achieved while retaining 93% of the protons in the phenylene group.

To obtain the best possible spectrum of the Pake splitting, BPA-*d*₆ was dissolved in perdeuterio-BPA to obtain the spectra shown in Figure 2. Here, the Pake line shape is apparent because of reduced intermolecular dipole-dipole interactions. The center spike in this spectrum arises from residual protons of the perdeuterio-BPA, which constitutes 85% of the sample by weight and has 2% residual protons. The residual protons in BPA-*d*₆ and perdeuterio-BPA were determined from proton and deuterium spectra of the dissolved polymers, and the simulations in Figure 2, specifically the intensity of the center spike, are consistent with the known level of residual protons.

The Pake splitting can be determined from simulations of the spectra in Figure 2 by folding a Pake pattern with either Gaussian or Lorentzian broadening. A decrease of 10% in the Pake splitting from the low-temperature limit to the high-temperature limit is indicated by the simulation, but this small decrease is comparable to the uncertainty in the simulation. A 10% decrease could reflect the presence of some wobble of the C₁C₄ axis, and such a wobble has been reported by Schaefer⁷ based upon carbon-proton dipolar rotational spin-echo line shapes of the methyl carbons in BPA. The persistence of the Pake splitting does allow for the rejection of one of the CSA line shape simulations, namely, rotation about an axis inclined

The angle Δ is between the internuclear vector and the axis of internal rotation.

The three bond jump segmental motion description can also be combined with a description of restricted anisotropic rotational diffusion (13-14). In this case, the composite spectral density equation is

$$\begin{aligned}
 J_1(\omega_1) = & 2\sum_{k=1}^S G_k \frac{A_{1k0}}{1 + \omega_1^2 \tau_{k0}^2} + \\
 & \frac{B}{\lambda^2} \{ [(1 - \cos 2\epsilon)^2 + \sin^2 2\epsilon] \frac{\tau_{k0}}{1 + \omega_1^2 \tau_{k0}^2} + \\
 & \frac{1}{2} \sum_{n=1}^{\infty} \{ \left[\frac{1 - \cos(\epsilon - n\pi)}{(1 - \frac{n\pi}{\lambda})} + \frac{1 - \cos(\epsilon + n\pi)}{(1 + \frac{n\pi}{\lambda})} \right]^2 + \\
 & \left[\frac{\sin(\epsilon - n\pi)}{(1 - \frac{n\pi}{\lambda})} + \frac{\sin(\epsilon + n\pi)}{(1 + \frac{n\pi}{\lambda})} \right]^2 \} \frac{\tau_{nk0}}{1 + \omega_1^2 \tau_{nk0}^2} \} + \quad (3) \\
 & \frac{C}{2\lambda^2} \{ \frac{1}{2} [(1 - \cos 2\epsilon)^2 + \sin^2 2\epsilon] \frac{\tau_{k0}}{1 + \omega_1^2 \tau_{k0}^2} + \\
 & \sum_{n=1}^{\infty} \{ \left[\frac{1 - \cos(2\epsilon - n\pi)}{(2 - \frac{n\pi}{\lambda})} + \frac{1 - \cos(2\epsilon + n\pi)}{(2 + \frac{n\pi}{\lambda})} \right]^2 + \\
 & \left[\frac{\sin(2\epsilon - n\pi)}{(2 - \frac{n\pi}{\lambda})} + \frac{\sin(2\epsilon + n\pi)}{(2 + \frac{n\pi}{\lambda})} \right]^2 \} \frac{\tau_{nk0}}{1 + \omega_1^2 \tau_{nk0}^2} \} +
 \end{aligned}$$

where $\frac{1}{\tau_{k0}} = \frac{1}{\tau_k}$

$$\frac{1}{\tau_{nk0}} = \frac{1}{\tau_k} + \lambda_n \quad \text{and}$$

$$\lambda_n = \left(\frac{n\pi}{\lambda}\right)^2 \theta_{ir}$$

The new parameters for restricted anisotropic rotational diffusion are the angular amplitude over which rotation diffusion occurs, Δ , and the rotational diffusion coefficient for restricted anisotropic rotational diffusion, B_{ir} .

A second description of segmental motion can be combined with the various types of internal anisotropic internal rotation. Weber and Helland (5) characterize segmental motion in terms of a correlation time for single conformational transitions, τ_0 , and a correlation time for cooperative conformational transitions, τ_1 . This model has been applied to nuclear spin relaxation before (5) and the form of the spectral density for a composite segmental motion and anisotropic internal rotation is written

$$J_i(\omega_i) = AJ_{ia}(\tau_0, \tau_1, \omega_i) + BJ_{ib}(\tau_{b0}, \tau_1, \omega_i) + CJ_{ic}(\tau_{c0}, \tau_1, \omega_i)$$

$$A = (3 \cos^2 \Delta - 1)^2/4$$

$$B = 3 (\sin^2 2\Delta)/4 \quad (4)$$

$$C = 3(\sin^4 \Delta)/4$$

for stochastic diffusion

$$\tau_{b0}^{-1} = \tau_0^{-1} + \tau_{ir}^{-1}$$

$$\tau_{c0}^{-1} = \tau_0^{-1} + (\tau_{ir}/4)^{-1}$$

for a three bond jump

$$\tau_{b0}^{-1} = \tau_{c0}^{-1} = \tau_0^{-1} + \tau_{ir}^{-1}$$

The form of J_{ia} , J_{ib} and J_{ic} is the same as J_{ij} given below with τ_{ij} replaced by τ_0 , τ_{b0} and τ_{c0} respectively.

$$J_{ij}(\omega_i) = 2\{[(\tau_0^{-1})(\tau_0^{-1} + 2\tau_1^{-1}) - \omega_i^2]^2 + [2(\tau_0^{-1} + \tau_1^{-1}\omega_i)]^2\}^{-1/4}$$

$$\times \cos [1/2 \arctan(2(\tau_0^{-1} + \tau_1^{-1})\omega_i / \tau_0^{-1}(\tau_0^{-1} + 2\tau_1^{-1}) - \omega_i^2)]$$

This description of segmental motion can also be combined with restricted anisotropic rotational diffusion

$$\begin{aligned}
J_i(\omega_i) = & AJ_i^{01}(\omega_i) + \\
& \frac{B}{\lambda^2} \{ [(1 - \cos \lambda)^2 + \sin^2 \lambda] J_i^{01}(\omega_i) + \\
& \frac{1}{2} \sum_{n=1}^{\infty} \left[\frac{[1 - \cos(\lambda - n\pi)]}{(1 - \frac{n\pi}{\lambda})} + \frac{[1 - \cos(\lambda + n\pi)]}{(1 + \frac{n\pi}{\lambda})} \right]^2 + \\
& \left[\frac{\sin(\lambda - n\pi)}{(1 - \frac{n\pi}{\lambda})} + \frac{\sin(\lambda + n\pi)}{(1 + \frac{n\pi}{\lambda})} \right]^2 \} J_i^{\lambda n}(\omega_i) + \\
& \frac{C}{2\lambda^2} \{ \frac{1}{2} [(1 - \cos 2\lambda)^2 + \sin^2 2\lambda] J_i^{01}(\omega_i) + \\
& \sum_{n=1}^{\infty} \left[\frac{[1 - \cos(2\lambda - n\pi)]}{(2 - \frac{n\pi}{\lambda})} + \frac{[1 - \cos(2\lambda + n\pi)]}{(2 + \frac{n\pi}{\lambda})} \right]^2 + \\
& \left[\frac{\sin(2\lambda - n\pi)}{(2 - \frac{n\pi}{\lambda})} + \frac{\sin(2\lambda + n\pi)}{(2 + \frac{n\pi}{\lambda})} \right]^2 \} J_i^{\lambda n}(\omega_i) \} \quad (5)
\end{aligned}$$

where

$$\begin{aligned}
J_i^{01}(\omega_i) = & \{ (\tau_0^{-1}(\tau_{01}^{-1} + \tau_1^{-1}) - \omega_i^2)^2 + \\
& (2\tau_{01}^{-1}\omega_i)^2 \}^{-1/4} \times \cos \left\{ \frac{1}{2} \arctan \frac{2\tau_{01}^{-1}\omega_i}{\tau_0^{-1}(\tau_{01}^{-1} + \tau_1^{-1}) - \omega_i^2} \right\} \\
J_i^{\lambda n}(\omega_i) = & \{ [(\tau_0^{-1} + \lambda_n)(\tau_{01}^{-1} + \tau_1^{-1} + \lambda_n) - \omega_i^2]^2 + \\
& (2(\tau_{01}^{-1} + \lambda_n)\omega_i)^2 \}^{-1/4} \\
& \times \cos \left\{ \frac{1}{2} \arctan \frac{2(\tau_{01}^{-1} + \lambda_n)\omega_i}{(\tau_0^{-1} + \lambda_n)(\tau_{01}^{-1} + \tau_1^{-1} + \lambda_n) - \omega_i^2} \right\} \\
\tau_{01}^{-1} = & \tau_0^{-1} + \tau_1^{-1} \\
\lambda_n = & \left(\frac{n\pi}{\lambda} \right)^2 D_{1r}
\end{aligned}$$

All of the terms have been defined in eqs. 2-4.

To apply the models to the interpretation of the data, the approach developed for the polycarbonates will be followed. The phenyl proton T_1 's are interpreted first in terms of segmental motion. For these protons, the dipole-dipole interaction is parallel to the chain backbone and therefore relaxed only by segmental motion. In the three bond jump model the parameters τ_h and m are adjusted to account for phenyl proton data, and in the Weber-Helfand model the parameters τ_0 and τ_1 are adjusted. Table II contains the three bond jump parameters, and Table III, the Weber-Helfand model parameters. Both models can simulate the data within 10% which is equivalent to the experimental error.

Phenyl group rotation can be characterized from the phenyl carbon T_1 's by assuming the segmental description developed from the proton data (5). Either segmental model can be used, and the corresponding correlation times for internal rotation of the phenyl group by stochastic diffusion, τ_{irp} 's, are displayed in Table II and Table III. Again both approaches match the observed carbon-13 data within the 10% uncertainty.

Table II: Phenyl Group Motion Simulation Parameters Using the Three Bond Jump Model

$^{\circ}\text{C}$	m	τ_h (ns)	τ_{irp} (ns)
0	1	2.69	1.85
20	1	1.30	1.19
40	1	0.79	0.73
60	1	0.49	0.299
80	3	0.180	0.247
100	5	0.080	0.192
120	7	0.049	0.145
E_a (kJ/mole)		30	20
$\tau_{\infty} \times 10^{14}$ (s)		0.59	30
Correlation Coefficient		0.99	0.99

Table III: Phenyl Group Motion Simulation Parameters Using the Weber-Helfand Model

$^{\circ}\text{C}$	τ_1 (ns)	τ_0 (ns)	τ_{irp} (ns)
0	3.80	6.01	2.15
20	1.89	3.7	1.15
40	1.09	2.34	0.72
60	0.49	2.00	0.280
80	0.259	1.99	0.240
100	0.142	1.86	0.170
120	0.070	1.70	0.150
E_a (kJ/mole)	30	9	21
$\tau_{\infty} \times 10^{14}$ (s)	1.04	97×10^2	20
Correlation Coefficient	0.99	0.94	0.99

Now the interpretation diverges from the polycarbonate pattern as the formal group is considered. As mentioned, the structural analogue to the formal group in the polycarbonate is the carbonate group, and the latter cannot be directly studied by solution spin relaxation studies since it has no directly bonded protons. If the formal is first viewed independently from the phenyl group data, one might attempt to employ segmental motion descriptions alone since the formal group lies in the backbone. Pursuing this approach, both the three bond jump and the Weber-Helfand models were applied to simulate the proton and carbon-13 data in Table I. Neither model is able to account for the data, with systematic discrepancies up to 70% in both attempts. The largest discrepancies occur at low temperatures with only somewhat better simulations possible at higher temperatures.

In one sense it is reassuring to determine that models for segmental motion cannot account for all data sets. On the other hand, it is still desirable to develop some description of motion which will account for the data at hand, since the failure to simulate implies some potentially interesting informational content. The successful phenyl group interpretation can assist the effort to account for the formal data. The segmental motion descriptions applied to the phenyl proton data are based on isotropic averaging of the dipole-dipole interactions by the segmental motion. One could assume that the same segmental motion description occurring at the phenyl groups also occurs at the formal group since both groups are adjacent in the backbone. If this assumption is made, some additional motion must be considered to match the observed formal relaxation times. In the context of the models being applied, the added motion could be an anisotropic rotation or restricted rotation. For the formal group, the first guess is rota-

tion or restricted rotation about the C-O axis. This would be a single backbone conformational transition occurring as an anisotropic motion on top of the segmental motion of say the Weber-Helfand model determined from the phenyl proton data. Complete anisotropic rotation about the C-O bond adequately accounts for the higher temperature data, but fails to simulate the lower temperature data by about 40%. A restricted rotation model at lower temperatures is also not able to simulate the observed T_1 's though it comes closer. Adding a rotation or restricted rotation about the C-O axis to the three bond jump model is equally unsuccessful as might be expected since so far the three bond jump and Weber-Helfand model have paralleled each other.

The next motion considered is rotation or restricted rotation of the OCH_2O unit about the O-O axis of the unit. The initial logic here was that the larger aromatic groups were slower moving anchors and the formal group was anisotropically rotating relative to the two oxygens which were the connections to the more sluggish phenyl groups. At higher temperatures, complete anisotropic rotation about the O-O axis in addition to a segmental motion description using the Weber-Helfand model developed from the phenyl proton data accounted for the formal data but discrepancies of 30% still remained at lower temperatures. The lower temperature data could be accounted for by allowing for incomplete anisotropic rotational diffusion about the O-O axis in addition to segmental motion. With complete rotation at higher temperatures and restricted rotation at lower temperatures, all formal proton and carbon-13 data can be simulated within the experimental uncertainty of the T_1 's. The anisotropic rotation simulation parameters are reported in Table IV for the case where segmental motion is characterized with the Weber-Helfand model on the basis of the phenyl proton data. A substitution of the three bond jump model for the Weber-Helfand model leads to nearly the same results.

Table IV: Formal Group Simulation Parameters Using the Weber-Helfand Model(a)

$^{\circ}\text{C}$	τ	$D_{\text{ir}} \times 10^{-10} \text{ (s}^{-1}\text{)}$
0	86	0.100
20	119	0.110
40	164	0.130
60	360	0.100
80	360	0.160
100	360	0.210
120	360	0.230

(a) The values of τ_1 and t_0 reported in Table III are used here as well as the parameters listed.

Discussion

As the first point, the dynamics of the phenyl group in the polyformal can be considered. Motional descriptions from the two segmental models can be compared as they have been before for the polycarbonates (5). In the three bond jump model the primary parameter is the harmonic mean correlation time, τ_h ; and in the Weber-Helfand model the primary parameter is the correlation time for cooperative backbone transitions, τ_l . At the lower temperatures studied, τ_0 plays an increasing role in the Weber-Helfand model but τ_l is still the major factor. This is an interesting point in itself since cooperative transitions were also found to predominate when the Weber-Helfand model was applied to the polycarbonates. Here in the polyformal, single bond conformational transitions do play a larger role; and this can be seen in the three bond jump model as well by the drop of m to 1 at lower temperatures. Since τ_l and τ_h are both measures of the time scale for cooperative motions, it is interesting to note that the Arrhenius summaries of the two correlation times in Tables II and III are very similar. This similarity, taken together with the domination of cooperative transitions in the interpretations, supports the utility of both models though the Weber-Helfand model is developed from a more detailed analysis of chain motion.

One interesting difference between the Weber-Helfand interpretation of the polyformal and the polycarbonates is the relative apparent activation energies for τ_l and τ_0 . For the polycarbonates, the activation energies for τ_0 and τ_l were about the same (5) as would be expected if the cooperative transitions occurred sequentially as opposed to simultaneously (15-17). For the polyformal, the activation energy for the cooperative process is much higher than for the single transitions which is more indicative of simultaneous cooperative transitions such as a crankshaft. Since the single transitions are minor processes in both the polycarbonates and to a lesser extent in the polyformal, dwelling on the activation energy differences may be risky.

It is worth noting that the description of phenyl group rotation is not significantly influenced by changing descriptions of segmental motion. This too supports the utility of both models and the validity of the general analysis of local motion for phenyl groups as being divided between segmental motion and internal rotation.

Segmental motion and phenyl group rotation in the polyformal can be compared to that of the polycarbonates. Relative to the analogous Chloral polycarbonate (5), the cooperative segmental motion in the polyformal is similar in general time scale but has a significantly higher activation energy. Phenyl group rotation in the polyformal and the polycarbonate are nearly identical. This suggests phenyl group rotation is a very localized process not greatly influenced by replacing the carbonate link with a formal link. On the other hand, it is hard to imagine phenyl group rota-

tion as a simple process within the bisphenol unit since MNDO calculations (18) indicate a high barrier within this unit.

Another interesting point about phenyl group rotation in the polyformal and polycarbonates is that it is best modeled in solution as stochastic diffusion rather than two fold jump (π flips). In solid BPA polycarbonate, both deuterium (19) and carbon-13 (20) lineshape analysis point to two fold jumps or π flips as the primary process. Calculations by Tonelli (21-22) also point to low barriers to phenyl group rotation for isolated BPA chains. If the intramolecular barrier for phenyl group rotation is indeed low as indicated by the solution studies and the calculations, the change to a higher barrier (6,18) and π flips in the solid must reflect intermolecular interactions. This is indeed plausible since the new conformation following a π flip in the solid requires no change in the surroundings (no change in free volume) yet the surroundings could provide an appreciable barrier to the transition.

As mentioned, the formal link provides new dynamic information relative to the polycarbonates where no detailed analysis of the carbonate unit is possible. In the interpretation, a rather complex description is required to account for the formal relaxation data. According to the interpretation, the formal group undergoes segmental motion as determined at the phenyl group plus anisotropic rotation about the oxygen-oxygen axis of the formal group. At low temperatures this anisotropic rotation is described as restricted rotational diffusion. The main question is whether there is any physical sense to such a picture. Since the segmental motion is somewhat cooperative and the phenyl group is adjacent, it seems reasonable to assume that this motion extends over both the phenyl and formal groups. The real question is the anisotropic restricted rotation. To pursue this aspect, conformational energy maps of dimethoxymethane were reviewed (23-24). The lowest conformations are gg' and g'g and this unusual situation relative to polyethylene chains is commonly called the anomeric effect. Each of these conformations has two conformations which are only 4kJ higher in energy. The tg' and gt conformations are energetically near the gg' conformation and the tg and g't conformations are energetically near the g'g conformation. The g'g', gg and tt states are considerably higher in energy. The most facile conformational changes from the lowest states could be represented by

$$\begin{aligned}tg' &= gg' = gt \\g't &= g'g = tg\end{aligned}\tag{6}$$

At lower temperatures where a given formal unit is likely to be either gg' or g'g, the transitions represented by eq. 6 would result in restricted rotational averaging. This would generally agree with the results obtained from the simulation of the formal relaxation data from 0 to 40 degrees where the angular amplitude

of restricted rotation, ℓ , ranges from 86 to 164 degrees. At higher temperatures populations in states other than gg' or $g'g$ would become larger allowing for the more common occurrence of conformational changes other than those listed in eq. 6. This would result in effectively complete rotation in agreement with the simulation from 60 to 120 degrees.

These arguments would account for the shift from restricted rotation to complete anisotropic rotation, but why is the choice of the oxygen-oxygen axis made? In fact, it can only be a rough approximation, since the ends of the formal group must move during these conformational changes. The time scale for the formal group conformational changes are only somewhat more rapid relative to the time scale of segmental motion and phenyl group rotation, so phenyl groups are only somewhat sluggish with respect to the formal group. A more detailed and accurate model for the formal group motion could be undertaken but the data in hand do not warrant it. The present picture points to single conformational transitions at the formal group which result in only partial spatial averaging of dipolar interactions at lower temperatures.

Acknowledgments

The research was carried out with financial support of National Science Foundation Grant DMR-790677, of National Science Foundation Equipment Grant No. CHE 77-09059, of National Science Foundation Grant No. DMR-8108679, and of the U.S. Army Research Office Grant DAAG 29-82-G-0001.

Literature Cited

- (1) A.A. Jones and R.P. Lubianez, *Macromolecules* (1978) 11, 126.
- (2) R.P. Lubianez, A.A. Jones and M. Bisceglia, *Macromolecules* (1980) 12, 1141.
- (3) A.A. Jones and M. Bisceglia, *Macromolecules* (1979) 12, 1136.
- (4) J.F. O'Gara, S.G. Desjardin and A.A. Jones, *Macromolecules* (1980) 13, 64.
- (5) J.J. Connolly, E. Gordon and A.A. Jones, submitted to *Macromolecules*.
- (6) A.F. Yee and S.A. Smith, *Macromolecules* (1981) 14, 54.
- (7) A.A. Jones and W.H. Stockmayer, *J. Polym. Sci., Polym. Phys. Ed.* (1977) 15, 847.
- (8) T.A. Weber and E. Helfand, submitted to *J. Chem. Phys.*

- (9) A.S. Hay, F.L. Williams, G.M. Loukes, H.M. Kelles, B.M. Boulette, P.E. Donohue and D.S. Johnson, *Polym. Prepr. Am. Chem. Soc. Div. Polym. Chem.* (1982) 23(2), 117.
- (10) A.A. Jones and M.F. Jarpey, unpublished results.
- (11) A.A. Jones, *J. Polym. Sci., Polym. Phys. Ed.* (1977) 15, 863.
- (12) D.E. Woessner, *J. Chem. Phys.* (1962) 36, 1.
- (13) W. Gronski and N. Murayama, *Makromol. Chem.* (1978) 179, 1521.
- (14) W. Gronski, *Makromol. Chem.* (1979) 180, 1119.
- (15) E. Helfand, *J. Chem. Phys.* (1971) 54, 4651.
- (16) E. Helfand, Z.R. Wasserman, and T.A. Weber, *Macromolecules* (1980) 13, 526.
- (17) J. Skolnik and E. Helfand, *J. Chem. Phys.* (1980) 72, 5489.
- (18) A.A. Jones, J.F. O'Gara, P.T. Inglefield, J.T. Bendler, A.F. Yee, and K.L. Ngai, *Macromolecules* (1983) 16, 658.
- (19) H.W. Spiess, *Colloid. Polym. Sci.* (1983) 261, 193.
- (20) P.T. Inglefield, R.M. Anici, J.F. O'Gara, C.-C. Hung and A.A. Jones, submitted to *Macromolecules*.
- (21) A.E. Tonelli, *Macromolecules* (1972) 5, 558.
- (22) A.E. Tonelli, *Macromolecules* (1973) 6, 503.
- (23) I. Tvaroska and T. Bleha, *J. Mol. Struct.* (1975) 24, 249.
- (24) G.A. Jeffrey and R. Taylor, *J. Comp. Chem.* 1 (1980) 99.

RECEIVED September 22, 1983

Reprinted from ACS Symposium Series No. 247
NMR and Macromolecules

James C. Kistall, Editor

Copyright 1984 by the American Chemical Society

Reprinted by permission of the copyright owner

TEMPERATURE DEPENDENCE OF PHENYL GROUP MOTION IN BPA FRM SOLID STATE CARBON-13 LINE SHAPES

by

A. A. Jones and J. F. O'Gara
Jeppson Laboratory
Department of Chemistry
Clark University
Worcester, MA 01610

P. T. Inglefield
Department of Chemistry
College of the Holy Cross
Worcester, MA 01610

INTRODUCTION

The polycarbonate of bisphenol-A (BPA) exhibits the commercially important property of good impact resistance over a temperature range more than 250° below the glass transition temperature (1). It is believed that the presence of molecular motions in the glassy state at low temperatures is an important factor in the determination of the origin of this physical property (2). Recent solid state NMR studies involving carbon-13 chemical shift anisotropy (CSA) line shapes (3) and deuterium quadrupolar line shapes (4) have defined the phenyl group motion in BPA. These results indicate that motion at 120°C takes place about the C₁C₄ axis in the form of jumps between two minima separated by 180° (π flips) in combination with a restricted angular rotation over $\pm 30^\circ$ around each minimum. These results agree well with predictions made by Williams and Flory based on the spatial configurations of the polycarbonate chain (5).

In this report, we extend the analysis of the CSA line shape for a phenyl carbon in BPA to determine the temperature dependence of the rate and amplitude of the phenyl group motion. This knowledge should help provide a basis on which one can develop a further understanding of the mechanical properties.

EXPERIMENTAL

The sample of bisphenol-A polymer, single site carbon-13 enriched (>90%) ortho to the carbonate was synthesized from enriched phenol (2-13C) obtained from KCR isotopes. The carbon-13 CSA spectra were obtained at 22.636 MHz using cross polarization and high power decoupling methods with a Bruker SXP 20-100 spectrometer. Typical spectra have been presented elsewhere (3) and will not be repeated in this report. Temperature control was maintained to within ± 2 K with a Bruker B-ST 100/70 temperature controller.

INTERPRETATION

The principal values of the shielding tensor were determined previously (3) by simulation from a spectra at -160°C ($\sigma_{11} = -17$, $\sigma_{22} = 52$, $\sigma_{33} = 175$ ppm on the CS₂ scale). Two approaches can then be utilized to model the molecular motion and simulate line shapes at the various temperatures.

First, one can easily simulate a line shape if the molecular reorientation occurs at a rapid rate by replacing the rigid shielding tensor with a tensor averaged over the geometry of the motion. The method involves transferring the chemical shift tensor in the principal axis system (σ_{ijk}) with the appropriate matrix (6) to a desired molecular axis system (σ'_{xyz}) where the x axis is selected as the axis about which the rotation takes place: $\sigma'_{xyz} = R\sigma_{ijk}R^{-1}$. Rotation about the x axis by an angle α gives $\sigma'_{xyz}(\alpha) = R_1\sigma'_{xyz}R_1^{-1}$ in a similar manner. The elements of the CSA tensor for flips and/or restricted rotations are then obtained by appropriate averaging and the corresponding line shape generated (5).

If the molecular motion occurs at a frequency comparable to the linewidth, the line shape may no longer be described by a tensor and the above approach will not work. One must use a model which allows for a molecular reorientation at an arbitrary rate. We make use of the equations developed by Mehring for a simple two site jump model for a CSA line

shape (6). In this model, there is a single time constant corresponding to the average residence time of a particular site. To simulate line shapes, one only needs to vary this time constant and the elements for the averaged tensor corresponding to a restricted rotation.

Using the interpretation of the geometry of phenyl motion at 120°C as a starting point one can simulate the temperature dependence. From +120°C to approximately 0°C the flips occur at a rapid rate and one can simulate the CSA line shapes by simply changing the amplitude of the restricted rotation. In the region from -20°C to -60°C one must also decrease the rate of the π flip process as the line shape is changing from being nearly axially symmetric to asymmetric. The jump rate as a function of temperature was estimated by comparing the theoretical and experimental spectra. An Arrhenius plot of these jump rates yields an apparent activation energy of 25.5 kJ/mol. for the flip process (Figure 1). This number should be treated with caution as it is determined from a sampling of only a few data points over a very small frequency range. Figure 2 provides a description of the temperature dependence of the restricted rotation behavior. A plot of the root mean square displacement versus $T^{\frac{1}{2}}$ shows a good linear dependence. The value of the root mean square displacement of $\pm 17^\circ$ at 120°C corresponds to the $\pm 30^\circ$ angular displacement. At -60°C, the root mean square displacement of $\pm 7^\circ$ corresponds to a $\pm 10^\circ$ angular displacement.

DISCUSSION

The two site jump model is a simplistic approach for modeling the time dependence of a molecular reorientation. Often when dealing with motion in polymer systems, one must invoke a distribution of correlation times to account for experimental data. However, the frequency range of the line shape data does not warrant such an approach. However, the apparent activation energy of the flip process derived from a single correlation time analysis may be in serious error.

The linear behavior of the root mean square displacement of the restricted rotation versus $T^{\frac{1}{2}}$ is attributed to a description of the motion as a classical harmonic oscillator (8). The potential energy is proportional to the square of the angular displacement, $U \propto \theta^2$. By invoking the virial theorem, the average potential energy can be set equal to the average kinetic energy and is proportional to the temperature, $\langle U \rangle \propto kT$. Therefore, the mean square angular displacement is proportional to the temperature, $\langle \theta^2 \rangle \propto T$.

ACKNOWLEDGEMENTS

We are grateful to Drs. P. D. McMaster, E. W. Byrnes, and J. Campbell for synthesis of the carbon-13 labelled monomer and polymer. The research was carried out with financial support of the U.S. Army Research Office Grant DAAG 29-82-90001, of National Science Foundation Equipment Grant No. CHE 77-09059, and of National Science Foundation Grant No. DMR-8108679.

REFERENCES

1. J. Heijboer, J. Polym. Sci. C, 16, 3755 (1968).
2. A.F. Yee and S.A. Smith, Macromolecules, 14, 54 (1981).
3. P.T. Inglefield, R.M. Amici, J.F. O'Gara, C.-C. Hung and A.A. Jones, Macromolecules (to appear 1983).
4. H.W. Spiess, Colloid Polym. Sci., 261, 193 (1983).
5. A.D. Williams and P.J. Flory, J. Polym. Sci. A-2, 6, 1945 (1968).
6. D. Slotfeldt-Ellingsen and H.A. Resing, J. Phys. Chem., 84, 2204 (1980).
7. M. Mehring, NMR Basic Princ. Prog., 11, 2nd ed. (1983).
8. W. Gronski and N. Murayama, Makromol. Chem., 179, 1521 (1978) and 180, 1119 (1979).

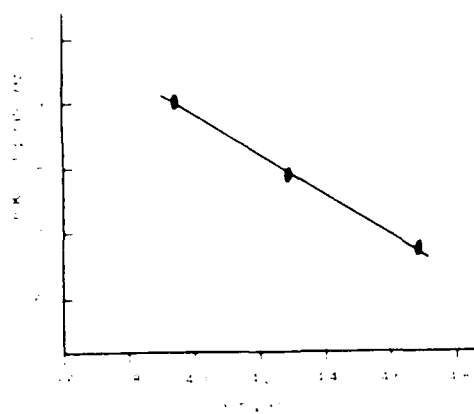


Figure 1. Variation of the flip rate versus temperature

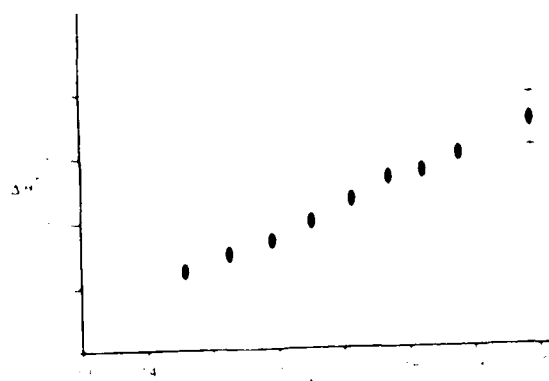


Figure 2. Variation of the flip rate versus temperature

A MOLECULAR LEVEL MODEL FOR MOTION AND RELAXATION
IN GLASSY POLYCARBONATE

Alan A. Jones

Department of Chemistry
Clark University
950 Main Street
Worcester, Massachusetts 01610

ABSTRACT

A local chain motion is proposed for the low temperature loss peak in heavy polycarbonate: namely a correlated conformational interchange between two neighboring carbonate units. One carbonate unit starts with a trans-trans conformation and the other with a cis-trans conformation. The interchange is produced by a rotation about one of the CO bonds in each of the carbonate units. The cis-trans conformation diffuses down the chain composed of largely trans-trans units by the repeated action of this process. The phenylene group attached to the other side of the carbonate unit from the rotating CO bond undergoes a π flip as rotation about the CO bond occurs through intermolecular couplings in the bulk polymer may also link the π flips to the interchange. This motion is consistent with existing solid state proton, carbon and deuterium line shape data on the phenylene group. It also agrees with the presence of a substantial dielectric and dynamical mechanical loss peak linked in time to the occurrence of π flips. This motion produces a volume fluctuation by translation of the bisphenol A unit between the rearranging carbonate units; and this volume fluctuation can diffuse down the polymer chain as the cis-trans conformation diffuses. Diffusion of a shape fluctuation and a volume fluctuation down the polymer chain is a process which could initiate the rapid relaxation of a macroscopic strain.

phenylene group. Thus the proposed motion is consistent with a large effect produced by phenylene group substitution ortho to the polycarbonate and lesser effect from substitution of the quaternary carbon at the BPA bridge head. Another structural modification, replacement of the carbonate by a formal group leads to a similar dynamic mechanical spectrum¹³ because the crucial CO bonds are present in both the carbonate and formal group though the geometry changes from about 120° to about 109° bond angles.

Lastly, the subject of impact resistance is considered. The polycarbonate of BPA shows good impact resistance over a wide range of temperatures.³¹ The diffusion of a conformation involving chain translation and an associated volume defect along the chain provides a mechanism at a molecular level which could lead to the rapid dissipation of a macroscopic strain. The diffusion along the chain to a large volume defect to relieve strain is also a promising proposal to reduce larger strains and would lead to the loss of good impact resistance in annealed samples again in agreement with observation.

motion could be thought of as a rotation about a single backbone bond with no subsequent compensating correlated motion. In this manner, new directions of backbone bonds are produced yielding the nearly isotropic spatial averaging observed at the glass transition. In an annealed sample, the diffusion process still takes place but the larger volume defects do not exist and the glass transition type segmental motions will not occur. The shoulder thus disappears in agreement with observation¹³.

The effect of structural modification on the dynamic mechanical spectrum also point to the key role of the CO bond in the carbonate unit. Substitution of the bridge group of the BPA unit has little effect on the low temperature loss peak¹³.

Substitution on the phenylene group at positions ortho to the carbonate shift the loss peak to higher temperature. For instance, the loss peak of the polycarbonate shown in figure 4 occurs 200° above the loss in BPA polycarbonate¹³. These ortho substitutions greatly increase steric interactions in the vicinity of the carbonate group and would tend to block rotation both about the CO carbonate bond and about the C₁C₁₁ axis of the

the shear loss which is physically reasonable since the small carbonate unit changes shape and the large BPA unit is moved so as to occupy a new volume. Volume fluctuations or relative motions of neighboring chains have been proposed before^{16,32} but no repeat unit level mechanism was suggested.

The amplitude of the bulk loss is reduced by cross-linking.³⁰ Volume fluctuations can be diffused along the chain by the cis-trans (or trans-cis), trans-trans interchange in the uncross-linked polymer but such volume fluctuation diffusion would be impeded by cross links leading to the diminished bulk loss in these systems.

In quenched polycarbonate samples, a low temperature shoulder (β relaxation) to the glass transition peak can be observed in the dynamic mechanical spectrum¹³. Larger volume defects may exist at some places in a quenched sample; and, with the proposed model, a localized strain could be diffused down the chain to the large volume defect. At this defect, segmental motions comparable to those of the glass transition could take place to relieve the strain. In this context, the glass transitions

a small amount as the cis-trans conformation diffuses along the chain which could lead to a larger loss. However, the computer simulations in polyethylene originally leading to the proposal of correlated segmental motions shows such process to be close in time but not simultaneous. The correlation function for dielectric loss and the magnitude of the dielectric loss under these circumstances is not known by the author; though further consideration of this aspect might be fruitful.

The dynamic mechanical loss would also be significant since a segmental motion involving two different conformations with different populations is involved. The carbonate unit changes shape which should lead to a shear loss and the BPA unit is translated which should lead to a volume fluctuation and bulk loss. The arguments for a complex correlation function and an indeterminate loss amplitude made for dielectric relaxation on the basis of the nature of correlated motion would also appear to apply to the mechanical problem as well. However, both a shear and bulk loss are reported³¹ and they occur at approximately the same frequency. The amplitude of the bulk loss is larger than

fact and may not change drastically with temperature. Further examination of the carbonate CSA line shape might be fruitful but would involve locating the principal axes for both the trans-trans and cis-trans conformations.

Dilute solution NMR relaxation data also show an apparent coupling or cooperativity between phenylene group rotation and segmental motion.²⁹ The solution data also indicate a preference for correlated segmental motions over a rotation about a single backbone bond²⁹ though both processes occur.

Dielectric loss would be substantial according to the model and linked to NMR data as is observed. The magnitude of the loss should be large since it involves both a partial reorientation of the carbonate group and a change from trans-trans to cis-trans (or trans-cis) conformation which could well have different dipole moments. On the other hand, the overall motion is an interchange of dipole moments associated with the carbonate units. If the interchange were simultaneous, only a small loss would appear likely since the carbonates and the BPA units are only slightly reoriented. Many repeat units could be reoriented

intramolecular and intermolecular in origin. The π flips would appear to be geometrically simple but in frequency the motion would appear complex since it is coupled to a segmental type of motion which diffuses along the chain. Thus, the geometric restrictions determined by proton, deuterium, carbon-13 CSA and carbon-13 dipolar line shapes and the broad T_1 and $T_{1\rho}$ relaxation minima²¹ are consistent with the proposed motion.

The most severe test of the model could have come from the carbon-13 anisotropy line shapes of the carbonate itself²⁰. Unfortunately the spectra are not decisive in either supporting or rejecting the model. As mentioned, the line shape is not strongly temperature dependent and the principal shielding axes are not well located. A further complication arises from the fact that the model proposes an interchange from a cis-trans (or trans-cis) to a trans-trans conformational which would imply that the observed line shape would actually be composed of two superimposed though probably similar shielding tensors line shapes. Since the trans-trans conformation is assumed to predominate, the carbonate CSA tensor would largely reflect this

tion function. An assumption of the model proposed here is that the life times of the states before and after the correlated motion composed of two rotations about CO bonds is long compared to the times between the two rotations. All of these motions are discussed in terms of isolated chains but the nature of the glass also strongly influences the correlation function.

RELATIONSHIPS OF THE MODEL TO RELAXATION DATA

The model can be compared to NMR data first since these results place the greatest restrictions on proposed motions. To begin with, the model is consistent with the preservation of the proton dipolar Pake doublet.¹⁶ The phenylene group undergoes flips about the C_1C_4 axis and translation but only about a 10° or less reorientation of the C_1C_4 axis corresponding to the virtual backbone bond. It is important that the CO rotation axis is nearly parallel to the C_1C_4 axis for there to be little C_1C_4 axis reorientation.²¹

The model includes " flips as a motion coupled to the isomerization of the carbonate unit. This coupling could be both

the left side of BPA units.

The motion proposed is a segmental motion but limited in nature. The BPA units are not significantly though slightly reoriented in space and would not be reoriented in the model until the glass transition is reached. The carbonate unit is reorienting but not isotropically and again isotropic rotational reorientation does not take place until the glass transition is reached. Single, uncorrelated backbone rotations producing conformational changes are the type of motion which would produce isotropic averaging and would be anticipated at the glass transition temperature, T_g .

In time, the proposed motion is complex. If bond directions of an individual carbonate unit are followed in an isolated chain, they would have a correlation function similar to that proposed by Helfand for correlated motion, the Bessel function of order zero. However, a compensating reorientation of a nearby carbonate unit occurs soon after the first reorientation. Thus the correlation function for dielectric loss under these circumstances would be more complex than the bond direction correla-

The virtue of the proposed correlated conformational change is that the chain ends do not have to translate. In this particular example in the polycarbonates, the bisphenol A (BPA) unit of the polymer is not significantly reoriented except for a flip of a phenylene group about the C_1C_4 axis. The one BPA unit between the two carbonates which interchange conformation is translated and slightly reoriented. This translation of a BPA unit can diffuse along the chain as the cis-trans or trans-cis unit migrates down the backbone; and this migration is typical of a diffusional motion along the backbone of the chain.

Note that there is only one type of motion in the sense that a cis-trans interchange with a trans-trans must be energetically equivalent with a trans-cis interchange with a trans-trans. However, the intramolecular coupling of one of these symmetry related motions is proposed to affect only the one of phenylene groups in a BPA unit. The other phenylene ring in a BPA unit is coupled to the other interchange. Referring to Figure 3, a trans-cis to trans-trans interchange flips rings on the right side of BPA units while a cis-trans to trans-trans

mational interchange.

The exchange of the cis-trans (or trans-cis) and trans-trans conformations is similar to the correlated conformational changes seen by Helfand²³⁻²⁶ in computer simulations of polyethylene chains. In the glassy solid the exchange of the conformations is likely to be more nearly correlated relative to dilute solution reflecting stronger intermolecular interactions. This would lead to barrier heights from one to two times the C-O bond rotation energy depending on the degree of correlation; though in the computer simulations of polyethylene, the barrier heights were found to be near one bond rotation energy. This C-O bond is found to have a low barrier,^{21,27,28} about 10 kJ, according to several theoretical calculations^{21,28}. The whole potential surface for polycarbonates for bond rotation consists of similarly low barriers²⁷ so compensating small distortions could aid the proposed conformational change; and, in addition, the high degree of motion in polycarbonate glass provides a more liquid like environment for a conformational change relative to most glassy polymers.

picture or model is qualitative though quantitatively consistent with geometric data from NMR line shape studies and leads to a mechanism for both a sizeable dielectric and mechanical loss.

MODEL

The model is relatively simple and is displayed in figure 3. The polycarbonate chain in the glass is composed of largely trans-trans units with respect to the carbonate group with an occasional cis-trans or trans-cis unit. The fundamental motion is the exchange of a cis-trans (or trans-cis) conformation of the carbonate with a trans-trans conformation of a neighboring carbonate. This exchange is produced by rotation about one of the CO bonds in each of two carbonate groups. As rotation about the CO carbonate group occurs the phenylene group attached to the other side of the same carbonate group flips about its C_1C_4 axis. The C_1C_4 axis and the CO carbonate bond direction on the other side of the carbonate group are nearly though not exactly parallel. Intermolecular coupling in the bulk polymer as well as intramolecular coupling could link the - flips to the confor-

shape changed little with temperature and the spatial orientation of the principal axes of the shielding tensor are not well-known for this group. The large dielectric loss can only be associated with motion of the carbonate group so it is quite unusual that the anisotropy study does not reflect the motion.

Both deuterium and carbon-13 dipolar line shape data are also available for the methyl groups^{18,19}. The spectra indicate methyl group rotation and possibly some small amount of backbone oscillation but no other major reorientation.

Relaxation maps have been prepared showing that proton spin relaxation, NMR line shape collapse, dielectric loss and dynamic mechanical loss are all at least phenomenologically related in time^{21,22}. Since the only clearly defined motion is π flips, legitimate questions have been raised as to how exchange of a symmetric group between two equivalent minima can produce a large mechanical loss. Also motion of the phenylene group will not account for dielectric relaxation.

It is the purpose of this report to propose a model which can draw various relaxation studies to a common picture. The

persistence of a dipolar splitting between adjacent phenylene protons up to the glass transition. This implied that the virtual bond corresponding to the phenylene group could not be reorientating in space. It did allow for either translation of the phenylene group or reorientation of the phenylene group about the C_1C_4 axis. This conclusion was later confirmed for the polycarbonate in figure 1 through observations on a partially deuterated form.¹⁷

Subsequent attention centered on the phenylene group and three solid state NMR experiments were performed to further determine the geometry of motion. The first report came from deuterium NMR¹⁸ which concluded that the phenylene group was undergoing π flips. Because the deuterium quadrupolar interaction is axially symmetric, some room for doubt remained. However, a carbon-13 carbon shift anisotropy study confirmed the π flip conclusion while eliminating other possibilities¹⁷; and a carbon-13 rotational dipolar study also came to the π flip conclusion¹⁹.

A carbon-13 chemical shift anisotropy line shape study has also been made on the carbonate carbon²⁰. However, the line

The local chain dynamics of glassy polycarbonate has intrigued many investigators over the past twenty-five years. Traditional experiments probing dielectric relaxation¹⁻⁸ and dynamic mechanical relaxation⁶⁻¹³ below the glass transition indicated large scale motion with very broad loss peaks at low temperatures (the gamma relaxation). These experiments were not suitable for defining the specific geometry of the motions in polycarbonate (figure 1) though certain implications from studies of a variety of structural analogs^{7,8,13} did provide useful information in developing proposals for motions. Wide-line NMR studies^{14,15} also observe relaxation effects below the glass transition; but the lack of structural specificity produced only general conclusions comparable to the dielectric and dynamic mechanical work.

Recently, more sophisticated solid state NMR line shape studies have provided some very detailed geometric information. The first definitive line shape result¹⁶ was obtained on a structural analog of BPA polycarbonate which contained only phenylene protons (figure 2). The proton spectrum showed the undiminished

CONCLUSION

Polycarbonate is a special system with generally low conformational barriers to rotation. The geometry of the carbonate unit allows for a process in which the large component of the repeat unit, EPA, is not appreciably reoriented while the small carbonate unit is reoriented. This is a partial segmental reorientation short of the isotropic segmental motion associated with glass transition. The model proposed here is quantitatively consistent with the geometric requirements of the NMR data. It is qualitatively consistent with the presence of significant dielectric and dynamic mechanical loss. It is also qualitatively consistent with broad loss peaks or relaxation minima since it is associated with a relatively complex motion: diffusion of a conformation along the chain backbone in a glassy solid. It couples the α flips to this more complex conformational change in agreement with relaxation maps²¹ though the flips are not the key motion contributing to the mechanical and dielectric properties. The model involves a process which could lead to long range dissipation of strain though it starts with a specific

local chain motion.

The data in hand do not absolutely lead to the motional model proposed here though they are consistent with it. The leading alternative motional model would be oscillation of the BPA unit and the carbonate unit. Certainly such oscillation exists. The phenylene group data displays this motion in addition to flips and Henrichs²⁰ favors oscillation as the best explanation of the carbonate CSA data. However, it is hard for this author to see how an oscillation of the order of $\pm 20^\circ$ at room temperature can lead to the large mechanical and dielectric losses observed in BPA polycarbonate. A jump between two different states with unequal populations separated by a barrier seems a more plausible mechanism for large losses.

The role of intermolecular couplings versus intramolecular coupling in the proposed motion is not entirely clear. Certain motions can be argued to be unlikely based on intermolecular interactions. For instance, rotation of the two rings and bridgehead as a unit about the oxygen-oxygen axis is unlikely because it would sweep out a large volume thus involving sig-

nificant intermolecular interactions in the bulk. The motion proposed here reorients only the small carbonate group as opposed to the whole BPA unit. The phenylene group motion of π flips involves no net reorientation and requires a much smaller fluctuation in the surroundings. The BPA unit is translated as a whole in the proposed motion which corresponds to a very specific motion which may lead to experimentally testable consequences. The separation of the relative role of intramolecular and intermolecular interactions in the coupling of π flips to the cis-trans (or trans-cis) to trans-trans interchange is unresolved. The π flips are proposed to be coupled by both factors but the relative importance is not easily assessed. In any case, it is hoped that the act of proposing this model will lead to new quantitative tests which can discriminate more decisively among possible models.

ACKNOWLEDGEMENT

The author thanks Drs. John T. Bendler, Albert F. Yee and P.T. Inglefield for many helpful discussions. The thesis of John

F. O'Gara led to a reconsideration of the whole of polycarbonate dynamics and the proposed motion. The research was carried out with the financial support of National Science Foundation Grant DMR-790677, and of the U.S. Army Research Office Grant DAAG 29-82-G-0001.

References

1. Krum, F.; Muller, F., Kolloid-Z. 1959, 164, 81.
2. Muller, F.; Huff, K., Kolloid-Z. 1959, 164, 34.
3. Krum, F., Kolloid-Z. 1959, 165, 77.
4. Matsuoka, S.; Ishida, Y., J. Polym. Sci. 1966, Part C, 14, 247.
5. Pochan, J.M.; Ginon, H.W.; Froix, M.J.; Hinman, D.F.,
Macromolecules 1978, 11, 165.
6. Schnell, H. "Chemistry and Physics of Polycarbonates,"
John Wiley and Sons, New York, 1964.
7. Massa, D.J.; Flick, J.R., Poly. Prepr., Am. Chem. Soc.,
Div. Polym. Chem. 1973, 14 (2), 1249.
8. Massa, D.J.; Rusanowsky, F.P., Polym. Prepr., Am. Chem.
Soc., Div. Polym. Chem. 1976, 17 (2), 184.
9. Illers, K.; Breuer, H., Kolloid-Z. 1961, 176, 110.
10. Reding, F.P.; Faucher, J.A.; Whitman, R.D., J. Polym. Sci.
1961, 54, 356.
11. Zutty, N.L.; Reding, F.P.; Faucher, J.A., J. Polym. Sci.

1962, 62, S171.

12. Mikhaolov, G.R.; Edelant, M.P., Vysokmol. Soedin. 1950,

2, 287.

13. Yee, A.F.; Smith, S.A., Macromolecules 1981, 14, 54.

14. Garfield, L.F., J. Polym. Sci., Part C 1970, 30, 551.

15. Davenport, R.A.; Manuel, A.J., Polymer 1977, 18, 557.

16. Inglefield, P.T.; Jones, A.A.; Lubianez, R.P.; O'Gara, J.F.,

Macromolecules 1981, 14, 288.

17. Inglefield, P.T.; Amici, R.M.; O'Gara, J.F.; Hung, C.-C.;

Jones, A.A., Macromolecules 1983, 16, 1552.

18. Spiess, H.W., Colloid Polym. 1983, 261, 193.

19. Schaefer, J.; Sefeik, M.D.; Stejskal, E.O.; McKay, R.A.;

Dixon, W.J.; Cais, R.E., Prepr. Div. Org. Coat. Plast. Chem.

1983, 48, 87.

20. Henrichs, P.M.; Linder, M.; Hewitt, J.M.; Massa, D.;

Isaacson, H.V., Macromolecules, in press.

21. Jones, A.A.; O'Gara, J.F.; Inglefield, P.T.; Bendler, J.T.;

Yee, A.F.; and Ngai, K.L., Macromolecules 1983, 16, 658.

22. Jones, A.A.; O'Gara, J.F.; Inglefield, P.T., Polym. Prepr.,

- Am. Chem. Soc., Div. Polym. Chem. 1984, 25(1), 345.
23. Helfand, E.; Wasserman, Z.R.; Weber, T.A., *Macromolecules* 1980, 13, 526.
24. Skolnick, J.; Helfand, E., *J. Chem. Phys.* 1980, 72, 5489.
25. Hall, C.K.; Helfand, E., *J. Chem. Phys.* 1982, 77, 3275.
26. Weber, T.A.; Helfand, E., *J. Phys. Chem.* 1983, 87, 2891.
27. (a) Tonelli, A.E., *Macromolecules* 1972, 5, 558.
(b) Tonelli, A.E., *Macromolecules* 1973, 6, 503.
28. Bendler, J.T., *Ann. N.Y. Acad. Sci.* 1981, 371, 299.
29. Connolly, J.J.; Gordon, E.; Jones, A.A., *Macromolecules*, in press.
30. Yee, A.F., *Polym. Prepr., Am. Chem. Soc., Div. Polym. Chem.* 1981, 22(2), 285.
31. Heijboer, J., *J. Polym. Sci., Part C* 1968, 16, 3755.
32. Schaefer, J.; Stejskal, E.O.; McKay, R.A., *Polym. Prepr., Am. Chem. Soc., Div. Polym. Chem.* 1984, 25(1), 342.
33. Williams, A.D.; Flory, P.J., *J. Polym. Sci., Part A-2* 1968, 6, 1945.

Figure 1: The Chloral Polycarbonate Repeat Unit:

An Analogue of BPA Polycarbonate.

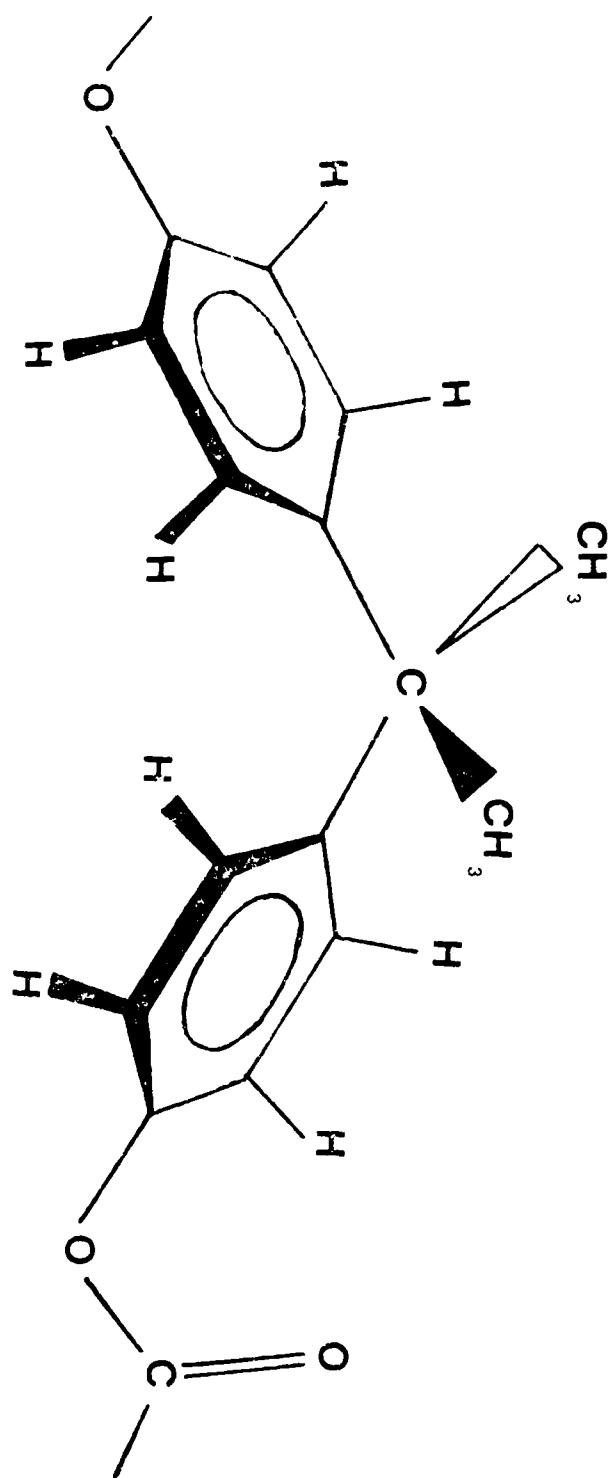
Figure 2: The BPA Polycarbonate Repeat Unit.

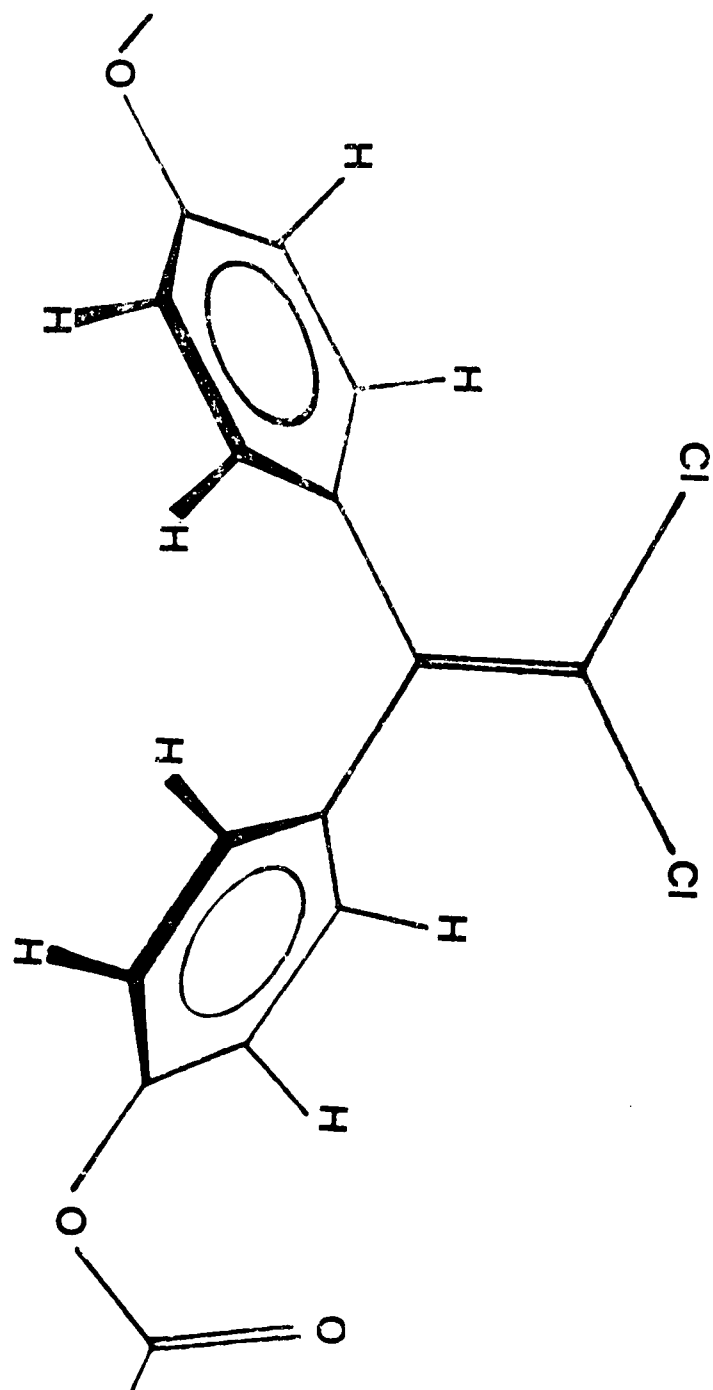
Figure 3: BPA Polycarbonate Chains.

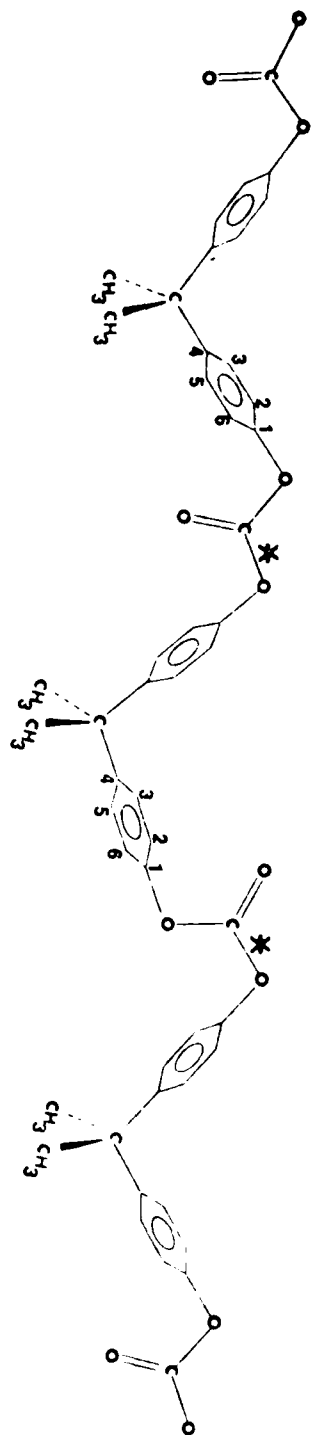
The carbonate CO bonds with asterisks indicate points of bond rotation. The phenylene rings undergoing flips in association with the CO bond rotations are numbered. The correlated conformational change from the top chain to the lower chain involves two neighboring carbonate groups and is produced by the CO rotations which interchange the trans-trans and trans-cis conformations. Note that the choice of a trans-cis unit in the figure is arbitrary. If a cis-trans unit were used the other phenylene rings would be flipped so over a period of time all rings

could be flipped as the cis-trans and trans-cis conformations diffuse along the chain. Conventional bond angles of 109° are used for all backbone bonds except the carbonate bond which are set at 120° . These choices lead to an 11° change in the C_1C_4 axis of the phenylene groups in the BPA unit between the carbonate units undergoing conformational change. If the bond angle suggested by Flory and Williams³³ are employed, the C_1C_4 reorientation of the phenylene group is less than 11° .

Figure 4: A Substituted Polycarbonate Repeat Unit.





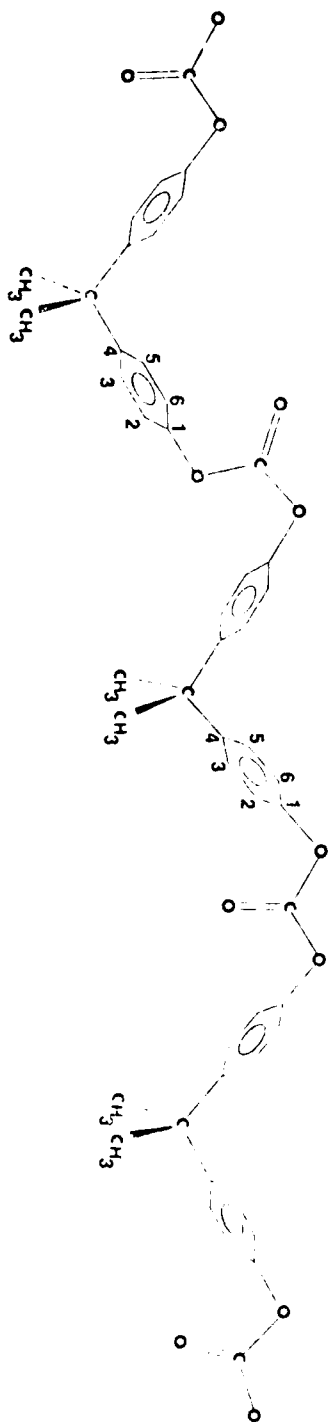


TRANS-TRANS

TRANS-TRANS

TRANS-CIS

TRANS-TRANS

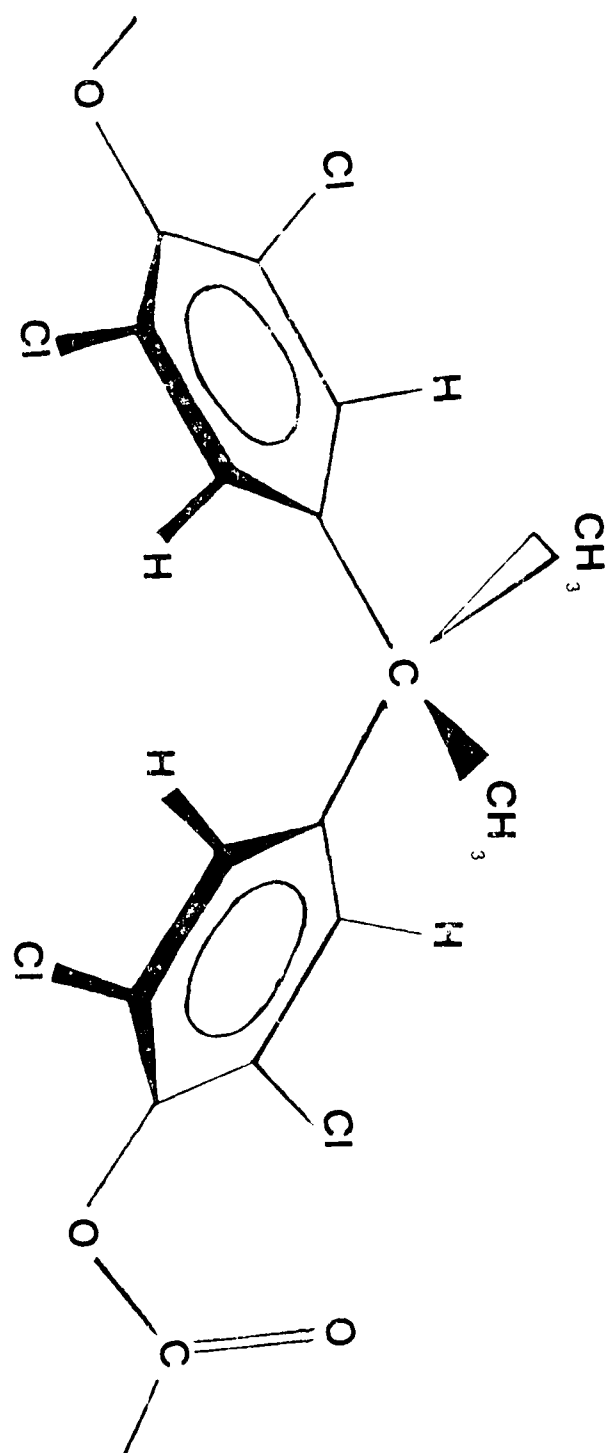


TRANS-TRANS

TRANS-CIS

TRANS-TRANS

TRANS-TRANS



Department of Psychology
University of Illinois at Chicago
Chicago, IL 60607
Worcester, MA 01601

1. 2. 3. 4. 5. 6. 7. 8. 9. 10. 11. 12. 13. 14. 15. 16. 17. 18. 19. 20. 21. 22. 23. 24. 25. 26. 27. 28. 29. 30. 31. 32. 33. 34. 35. 36. 37. 38. 39. 40. 41. 42. 43. 44. 45. 46. 47. 48. 49. 50. 51. 52. 53. 54. 55. 56. 57. 58. 59. 60. 61. 62. 63. 64. 65. 66. 67. 68. 69. 70. 71. 72. 73. 74. 75. 76. 77. 78. 79. 80. 81. 82. 83. 84. 85. 86. 87. 88. 89. 90. 91. 92. 93. 94. 95. 96. 97. 98. 99. 100. 101. 102. 103. 104. 105. 106. 107. 108. 109. 110. 111. 112. 113. 114. 115. 116. 117. 118. 119. 120. 121. 122. 123. 124. 125. 126. 127. 128. 129. 130. 131. 132. 133. 134. 135. 136. 137. 138. 139. 140. 141. 142. 143. 144. 145. 146. 147. 148. 149. 150. 151. 152. 153. 154. 155. 156. 157. 158. 159. 160. 161. 162. 163. 164. 165. 166. 167. 168. 169. 170. 171. 172. 173. 174. 175. 176. 177. 178. 179. 180. 181. 182. 183. 184. 185. 186. 187. 188. 189. 190. 191. 192. 193. 194. 195. 196. 197. 198. 199. 200. 201. 202. 203. 204. 205. 206. 207. 208. 209. 210. 211. 212. 213. 214. 215. 216. 217. 218. 219. 220. 221. 222. 223. 224. 225. 226. 227. 228. 229. 230. 231. 232. 233. 234. 235. 236. 237. 238. 239. 240. 241. 242. 243. 244. 245. 246. 247. 248. 249. 250. 251. 252. 253. 254. 255. 256. 257. 258. 259. 260. 261. 262. 263. 264. 265. 266. 267. 268. 269. 270. 271. 272. 273. 274. 275. 276. 277. 278. 279. 280. 281. 282. 283. 284. 285. 286. 287. 288. 289. 290. 291. 292. 293. 294. 295. 296. 297. 298. 299. 300. 301. 302. 303. 304. 305. 306. 307. 308. 309. 310. 311. 312. 313. 314. 315. 316. 317. 318. 319. 320. 321. 322. 323. 324. 325. 326. 327. 328. 329. 330. 331. 332. 333. 334. 335. 336. 337. 338. 339. 340. 341. 342. 343. 344. 345. 346. 347. 348. 349. 350. 351. 352. 353. 354. 355. 356. 357. 358. 359. 360. 361. 362. 363. 364. 365. 366. 367. 368. 369. 370. 371. 372. 373. 374. 375. 376. 377. 378. 379. 380. 381. 382. 383. 384. 385. 386. 387. 388. 389. 390. 391. 392. 393. 394. 395. 396. 397. 398. 399. 400. 401. 402. 403. 404. 405. 406. 407. 408. 409. 410. 411. 412. 413. 414. 415. 416. 417. 418. 419. 420. 421. 422. 423. 424. 425. 426. 427. 428. 429. 430. 431. 432. 433. 434. 435. 436. 437. 438. 439. 440. 441. 442. 443. 444. 445. 446. 447. 448. 449. 450. 451. 452. 453. 454. 455. 456. 457. 458. 459. 460. 461. 462. 463. 464. 465. 466. 467. 468. 469. 470. 471. 472. 473. 474. 475. 476. 477. 478. 479. 480. 481. 482. 483. 484. 485. 486. 487. 488. 489. 490. 491. 492. 493. 494. 495. 496. 497. 498. 499. 500. 501. 502. 503. 504. 505. 506. 507. 508. 509. 510. 511. 512. 513. 514. 515. 516. 517. 518. 519. 520. 521. 522. 523. 524. 525. 526. 527. 528. 529. 530. 531. 532. 533. 534. 535. 536. 537. 538. 539. 540. 541. 542. 543. 544. 545. 546. 547. 548. 549. 550. 551. 552. 553. 554. 555. 556. 557. 558. 559. 560. 561. 562. 563. 564. 565. 566. 567. 568. 569. 570. 571. 572. 573. 574. 575. 576. 577. 578. 579. 580. 581. 582. 583. 584. 585. 586. 587. 588. 589. 590. 591. 592. 593. 594. 595. 596. 597. 598. 599. 600. 601. 602. 603. 604. 605. 606. 607. 608. 609. 610. 611. 612. 613. 614. 615. 616. 617. 618. 619. 620. 621. 622. 623. 624. 625. 626. 627. 628. 629. 630. 631. 632. 633. 634. 635. 636. 637. 638. 639. 640. 641. 642. 643. 644. 645. 646. 647. 648. 649. 650. 651. 652. 653. 654. 655. 656. 657. 658. 659. 660. 661. 662. 663. 664. 665. 666. 667. 668. 669. 670. 671. 672. 673. 674. 675. 676. 677. 678. 679. 680. 681. 682. 683. 684. 685. 686. 687. 688. 689. 690. 691. 692. 693. 694. 695. 696. 697. 698. 699. 700. 701. 702. 703. 704. 705. 706. 707. 708. 709. 710. 711. 712. 713. 714. 715. 716. 717. 718. 719. 720. 721. 722. 723. 724. 725. 726. 727. 728. 729. 730. 731. 732. 733. 734. 735. 736. 737. 738. 739. 740. 741. 742. 743. 744. 745. 746. 747. 748. 749. 750. 751. 752. 753. 754. 755. 756. 757. 758. 759. 760. 761. 762. 763. 764. 765. 766. 767. 768. 769. 770. 771. 772. 773. 774. 775. 776. 777. 778. 779. 780. 781. 782. 783. 784. 785. 786. 787. 788. 789. 790. 791. 792. 793. 794. 795. 796. 797. 798. 799. 800. 801. 802. 803. 804. 805. 806. 807. 808. 809. 810. 811. 812. 813. 814. 815. 816. 817. 818. 819. 820. 821. 822. 823. 824. 825. 826. 827. 828. 829. 830. 831. 832. 833. 834. 835. 836. 837. 838. 839. 840. 84

1. *Journal of the American Medical Association*, 1997; 278: 1039-1044.

[illegible]

a further test).

Figure 1

five green-propylhaw cycles to remove the dissolved

1998, 1999, 2000, 2001, 2002, 2003, 2004, 2005, 2006, 2007, 2008, 2009, 2010, 2011, 2012, 2013, 2014, 2015, 2016, 2017, 2018, 2019, 2020, 2021, 2022, 2023, 2024, 2025, 2026, 2027, 2028, 2029, 2030, 2031, 2032, 2033, 2034, 2035, 2036, 2037, 2038, 2039, 2040, 2041, 2042, 2043, 2044, 2045, 2046, 2047, 2048, 2049, 2050, 2051, 2052, 2053, 2054, 2055, 2056, 2057, 2058, 2059, 2060, 2061, 2062, 2063, 2064, 2065, 2066, 2067, 2068, 2069, 2070, 2071, 2072, 2073, 2074, 2075, 2076, 2077, 2078, 2079, 2080, 2081, 2082, 2083, 2084, 2085, 2086, 2087, 2088, 2089, 2090, 2091, 2092, 2093, 2094, 2095, 2096, 2097, 2098, 2099, 2100, 2101, 2102, 2103, 2104, 2105, 2106, 2107, 2108, 2109, 2110, 2111, 2112, 2113, 2114, 2115, 2116, 2117, 2118, 2119, 2120, 2121, 2122, 2123, 2124, 2125, 2126, 2127, 2128, 2129, 2130, 2131, 2132, 2133, 2134, 2135, 2136, 2137, 2138, 2139, 2140, 2141, 2142, 2143, 2144, 2145, 2146, 2147, 2148, 2149, 2150, 2151, 2152, 2153, 2154, 2155, 2156, 2157, 2158, 2159, 2160, 2161, 2162, 2163, 2164, 2165, 2166, 2167, 2168, 2169, 2170, 2171, 2172, 2173, 2174, 2175, 2176, 2177, 2178, 2179, 2180, 2181, 2182, 2183, 2184, 2185, 2186, 2187, 2188, 2189, 2190, 2191, 2192, 2193, 2194, 2195, 2196, 2197, 2198, 2199, 2200, 2201, 2202, 2203, 2204, 2205, 2206, 2207, 2208, 2209, 2210, 2211, 2212, 2213, 2214, 2215, 2216, 2217, 2218, 2219, 2220, 2221, 2222, 2223, 2224, 2225, 2226, 2227, 2228, 2229, 2230, 2231, 2232, 2233, 2234, 2235, 2236, 2237, 2238, 2239, 2240, 2241, 2242, 2243, 2244, 2245, 2246, 2247, 2248, 2249, 2250, 2251, 2252, 2253, 2254, 2255, 2256, 2257, 2258, 2259, 2260, 2261, 2262, 2263, 2264, 2265, 2266, 2267, 2268, 2269, 2270, 2271, 2272, 2273, 2274, 2275, 2276, 2277, 2278, 2279, 2280, 2281, 2282, 2283, 2284, 2285, 2286, 2287, 2288, 2289, 2290, 2291, 2292, 2293, 2294, 2295, 2296, 2297, 2298, 2299, 2300, 2301, 2302, 2303, 2304, 2305, 2306, 2307, 2308, 2309, 2310, 2311, 2312, 2313, 2314, 2315, 2316, 2317, 2318, 2319, 2320, 2321, 2322, 2323, 2324, 2325, 2326, 2327, 2328, 2329, 2330, 2331, 2332, 2333, 2334, 2335, 2336, 2337, 2338, 2339, 2340, 2341, 2342, 2343, 2344, 2345, 2346, 2347, 2348, 2349, 2350, 2351, 2352, 2353, 2354, 2355, 2356, 2357, 2358, 2359, 2360, 2361, 2362, 2363, 2364, 2365, 2366, 2367, 2368, 2369, 2370, 2371, 2372, 2373, 2374, 2375, 2376, 2377, 2378, 2379, 2380, 2381, 2382, 2383, 2384, 2385, 2386, 2387, 2388, 2389, 2390, 2391, 2392, 2393, 2394, 2395, 2396, 2397, 2398, 2399, 2400, 2401, 2402, 2403, 2404, 2405, 2406, 2407, 2408, 2409, 2410, 2411, 2412, 2413, 2414, 2415, 2416, 2417, 2418, 2419, 2420, 2421, 2422, 2423, 2424, 2425, 2426, 2427, 2428, 2429, 2430, 2431, 2432, 2433, 2434, 2435, 2436, 2437, 2438, 2439, 2440, 2441, 2442, 2443, 2444, 2445, 2446, 2447, 2448, 2449, 2450, 2451, 2452, 2453, 2454, 2455, 2456, 2457, 2458, 2459, 2460, 2461, 2462, 2463, 2464, 2465, 2466, 2467, 2468, 2469, 2470, 2471, 2472, 2473, 2474, 2475, 2476, 2477, 2478, 2479, 2480, 2481, 2482, 2483, 2484, 2485, 2486, 2487, 2488, 2489, 2490, 2491, 2492, 2493, 2494, 2495, 2496, 2497, 2498, 2499, 2500, 2501, 2502, 2503, 2504, 2505, 2506, 2507, 2508, 2509, 2510, 2511, 2512, 2513, 2514, 2515, 2516, 2517, 2518, 2519, 2520, 2521, 2522, 2523, 2524, 2525, 2526, 2527, 2528, 2529, 2530, 2531, 2532, 2533, 2534, 2535, 2536, 2537, 2538, 2539, 2540, 2541, 2542, 2543, 2544, 2545, 2546, 2547, 2548, 2549, 2550, 2551, 2552, 2553, 2554, 2555, 2556, 2557, 2558, 2559, 2560, 2561, 2562, 2563, 2564, 2565, 2566, 2567, 2568, 2569, 2570, 2571, 2572, 2573, 2574, 2575, 2576, 2577, 2578, 2579, 2580, 2581, 2582, 2583, 2584, 2585, 2586, 2587, 2588, 2589, 2590, 2591, 2592, 2593, 2594, 2595, 2596, 2597, 2598, 2599, 2600, 2601, 2602, 2603, 2604, 2605, 2606, 2607, 2608, 2609, 2610, 2611, 2612, 2613, 2614, 2615, 2616, 2617, 2618, 2619, 2620, 2621, 2622, 2623, 2624, 2625, 2626, 2627, 2628, 2629, 2630, 2631, 2632, 2633, 2634, 2635, 2636, 2637, 2638, 2639, 2640, 2641, 2642, 2643, 2644, 2645, 2646, 2647, 2648, 2649, 2650, 2651, 2652, 2653, 2654, 2655, 2656, 2657, 2658, 2659, 2660, 2661, 2662, 2663, 2664, 2665, 2666, 2667, 2668, 2669, 2670, 2671, 2672, 2673, 2674, 2675, 2676, 2677, 2678, 2679, 26

1000 1000 1000 1000

[The following information was obtained from the file maintained by the FBI in connection with the investigation of the activities of the Communist Party, USA, District of Columbia Chapter.]

$$d_{\text{eff}} = d \left(1 + \frac{1}{2} \frac{d}{\lambda} \right) \quad \text{for } \frac{d}{\lambda} \ll 1 \quad \text{and} \quad d_{\text{eff}} = d \left(1 + \frac{1}{2} \frac{d}{\lambda} \right) \quad \text{for } \frac{d}{\lambda} \gg 1.$$
[illegible]

The function f is continuous on $[0, 1]$ and $f(0) = 0$, $f(1) = 1$. The function f is given by

1. *Journal of the American Medical Association*, 1990; 263: 1025-1026.

Measurement.

mental method, developed by Hall and Holland⁴, is

$$\phi(t) = \exp(-t/\tau_1) + \exp(-t/\tau_2) I_0(t/\tau_2) \quad (2)$$

Fourier transformation of the correlation function yields

$$\cos\left\{\frac{\pi}{2} \arctan 2(\tau_0^{-1} + \zeta^{-1}) \omega_0 \omega_1^{-1} (\tau_0^{-1} + 2\zeta^{-1}) - \omega_1\right\} \quad (3)$$

Jan. 1870.

times for 1990-1991 and 1991-1992 were previously employed

$$I(\omega) = \int d\omega P(\omega) I(\omega, \omega) \quad (13)$$

where $P(\omega) = (1/4\pi)$ and $d\omega = \sin\theta d\theta d\phi$. (A computer program which generates CSA line shapes on the basis of this model can be found in the Ph.D. thesis of Wemmer.²⁵)

In this approach, only a single correlation time is used to describe the flipping process. Starting with the 0°C line shape, we must decrease the rate of the π flip process with decreasing temperature as the line shape is changing in this region from being axially symmetric in shape to asymmetric. For most of this temperature region, the amplitude of the restricted rotation does not significantly alter the line shape and thus only the rate of the π flips controls the resultant line shape. However, the amplitude of the restricted rotation is estimated by extrapolation from the high temperature region. The π flip rate as a function of temperature is determined by comparing the theoretical and experimental spectra. A summary of line shape comparisons is contained in Figure 3 and the simulations are good with the possible exception of 0°C. At this temperature both the π flips and the restricted oscillation make comparable contributions to the line narrowing. When two motional processes induce roughly equivalent narrowing, difficulties in line shape simulation are encountered since neither can be assumed to be fast or dominant with respect to the other.²⁵

The results of these simulations are summarized as follows. An Arrhenius analysis of the single correlation times yields an apparent activation energy of 11 ± 5 kJ/mol for the flip process, as shown in Figure 4. This number should be treated with caution as it is determined from a sampling of only a few data points over a very small frequency range. Figure 5 is a plot of the root mean

arbitrary rate. We make use of the exchange model for a CSA line shape as described by Mehring²² and Wemmer.²⁵

The line shape equation for a multisite exchange where each site can exchange with any other site is given by

$$g(\omega) = (1/N) (L / (1 - KL))$$

where

(11)

$$L = \sum_{j=1}^N [i(\omega - \omega_j) - (1/T_{2j}) + NK]^{-1}$$

T_{2j} = spin-spin relaxation time

$K = \tau^{-1}$ = exchange or flipping rate

N = number of sites

ω_j = frequency of site j

$$\begin{aligned} \omega_j = & \sigma_{iso} + (\sigma_{33} - \sigma_{iso}) [P_2(\cos \beta) P_2(\cos \theta) + (3/4) \sin 2\theta \sin 2\beta \cos 2(\phi + \gamma) \\ & - 3 \sin \theta \cos \theta \sin \beta \cos \beta \cos(\phi + \gamma)] \\ & + ((\sigma_{11} - \sigma_{22})/2) [\sin 2\theta \cos 4\beta \cos(2(\phi + \gamma + \alpha)) + \sin 2\theta \sin 4\beta \cos(2(\phi + \gamma - \alpha)) \\ & + \sin \theta \cos \theta \sin \beta \{(\cos \beta + 1) \cos(\phi + \gamma + 2\alpha) + (\cos \beta - 1) \cos(\phi + \gamma + 2\alpha)\} \\ & + P_2(\cos \theta) \sin^2 \beta \cos(2\alpha)] \end{aligned}$$

and P_2 is the Legendre Polynomial. The Euler angles of the flipping axis with respect to the principal axis system of the tensor are (α, β, γ) and the Euler angles of the magnetic field with respect to the molecular frame containing the flipping axis as the z -axis are (β, γ) .

In NMR, the real part of $g(\omega)$ is termed the line shape $I(\omega)$.

$$I(\omega) = \text{Re } g(\omega) \quad (12)$$

This equation has been developed for a particular orientation of the molecular frame with respect to the magnetic field. For an isotropic powder sample, one has to average over all orientations

place about the C_1C_4 axis in the form of jumps between two minima separated by 180° (π flips) in combination with a restricted rotation over $\pm 30^\circ$ around each minimum. It should be noted here that there was a small ppm referencing problem in the earlier CSA study that was corrected here when interpreting the temperature dependence of the other CSA line shapes. The basic conclusions are the same although in the final modeling the restricted rotation occurs over a greater range, $\pm 36^\circ$, than previously reported for $+120^\circ\text{C}$. The oscillation is modeled as a restricted diffusion over an angular range using the square well potential.

Employing the interpretation of the geometry of the phenylene motion at $+120^\circ\text{C}$ as a starting point, one can simulate the temperature dependence of the changing CSA line shapes. From $+120$ to $+20^\circ\text{C}$, the π flips are in the limit of rapid motion as the line shapes can be described by a tensor and thus this molecular motion can still be modeled rather easily through the use of Euler transformation matrices and the appropriate angular weighting functions. In this temperature region, the line shapes are all of the same general shape as observed at $+120^\circ\text{C}$, although the σ_{11} and σ_{33} components of the averaged tensor move to make the spectra slightly broader as temperature decreases. One can simulate this line shape behavior, first, by assuming the π flips are occurring at a rapid rate and, second, by simply decreasing the amplitude of the restricted rotation with temperature.

If the molecular motion occurs at a frequency comparable to the spectral width the line shape may no longer be described by the above approach. For the spectra from 0 to -100°C , one can no longer assume that the π flips are occurring at a rapid rate and thus one must use a model which allows for an

The method of averaging depends on the potential function chosen to describe how the molecule is allowed to spend time between the end points of its oscillations. For example, if one assumes a square well potential then one may calculate each tensor element of $\langle \sigma_{xyz} \rangle$ as follows

$$\langle \sigma_{xyz}(i,j) \rangle_{a'} = \int_{-a'/2}^{+a'/2} R(a') \cdot \sigma_{xyz}(i,j) R(a')^{-1} da' / \int_{-a'/2}^{+a'/2} da' \quad (9)$$

The resultant matrix $\langle \sigma_{xyz} \rangle_{a'}$ may then be diagonalized to obtain three new average values, σ_{11} , σ_{22} and σ_{33} which correspond to the averaged tensor. The characteristic line shape may then be calculated with the equation²³

$$I(\nu; \sigma_{11}, \sigma_{22}, \sigma_{33}, \Delta\nu) = \int_{-\infty}^{+\infty} I^0(\nu - \xi; \sigma_{11}, \sigma_{22}, \sigma_{33}) f(\xi; \Delta\nu) d\xi$$

For $\sigma_{33} \leq \nu < \sigma_{22}$

$$I^0(\nu; \sigma_{11}, \sigma_{22}, \sigma_{33}) = \pi^{-1} K(x) (\sigma_{11} - \nu)^{-0.5} (\sigma_{22} - \sigma_{33})^{-0.5}$$

$$x = (\sigma_{11} - \sigma_{22})(\nu - \sigma_{33}) / [(\sigma_{22} - \sigma_{33})(\sigma_{11} - \nu)]$$

For $\sigma_{22} < \nu \leq \sigma_{11}$

(10)

$$I^0(\nu; \sigma_{11}, \sigma_{22}, \sigma_{33}) = \pi^{-1} K(x) (\nu - \sigma_{33})^{-0.5} (\sigma_{11} - \sigma_{22})^{-0.5}$$

$$x = (\sigma_{11} - \nu)(\sigma_{22} - \sigma_{33}) / [(\nu - \sigma_{33})(\sigma_{11} - \sigma_{22})]$$

For $\nu < \sigma_{11}$, and $\nu > \sigma_{33}$

$$I^0(\nu; \sigma_{11}, \sigma_{22}, \sigma_{33}) = 0$$

And

$$K(x) = \int_0^{\pi/2} (1 - x^2 \sin^2 \Psi)^{-1} d\Psi$$

$$f = (\xi, \Delta\nu) = 1 / (1 + (2\xi/\Delta\nu)^2)$$

where f describes the Lorentzian line broadening of the chemical shift dispersion, I^0 and the carbon chemical shifts increase toward lower fields. In the earlier communication, we reported on comparisons of various line shapes generated on this basis with the high temperature line shape. It was found that the most probable motional model suggested that the phenylene motion takes

An appropriate orientation of the molecular motion axis frame places the x-axis parallel to the C₁C₄ axis of the phenylene group so

$$\underline{R}(\delta) = \begin{vmatrix} \cos \delta & -\sin \delta & 0 \\ \sin \delta & \cos \delta & 0 \\ 0 & 0 & 1 \end{vmatrix} \quad (4)$$

with $\delta=60^\circ$ for the labelled carbon of interest. The shielding tensor in the molecular motion axis system σ_{xyz} is then given by

$$\underline{\sigma}_{xyz} = \underline{R}(\delta) \cdot \underline{\sigma}_{123} \cdot \underline{R}(\delta)^{-1}$$

One can now model the effect on the shielding of different motions of the phenylene group about the C₁C₄ axis. For instance, rotating the molecule about the x-axis by angle α' is defined by

$$\underline{\sigma}_{xyz}(\alpha') = \underline{R}(\alpha') \cdot \underline{\sigma}_{xyz} \cdot \underline{R}(\alpha')^{-1}$$

where

(6)

$$\underline{R}(\alpha') = \begin{vmatrix} 1 & 0 & 0 \\ 0 & \cos \alpha' & -\sin \alpha' \\ 0 & \sin \alpha' & \cos \alpha' \end{vmatrix} .$$

For rapid flipping of the phenylene group between two angular positions, separated by an angle α' , the motionally averaged shielding tensor, σ_{flip} , is given by

$$\underline{\sigma}_{flip} = (1/2)(\underline{\sigma}_{xyz} + \underline{\sigma}_{xyz}(\alpha')) \quad (7)$$

Another possible type of molecular reorientation that we may consider is rapid phenylene group rotation about the x-axis through all angular positions or through a limited angular range. We can model this type of motion by averaging over $\underline{\sigma}$ in equation 6.

$$\langle \underline{\sigma}_{xyz} \rangle_{\alpha'} = \langle \underline{R}(\alpha') \cdot \underline{\sigma}_{xyz} \cdot \underline{R}(\alpha')^{-1} \rangle_{\alpha'} \quad (8)$$

-160°C spectrum. At this temperature we can assume that the molecular re-orientation occurs at a rapid rate, where rapid means the correlation time is much shorter than the inverse of the spectral width involved. Thus we can calculate line shapes very simply by replacing the rigid shielding tensor with a tensor averaged over the geometry of the motion through the use of Euler transformation matrices and the appropriate angular weighting functions as outlined by Slotfeldt-Ellingsen and Resing²⁴ and Wemmer et al.^{25,26}

In this calculation one begins with the shielding tensor, $\underline{\sigma}_{123}$, in the principal axis system

$$\underline{\sigma}_{123} = \begin{bmatrix} \sigma_{11} & 0 & 0 \\ 0 & \sigma_{22} & 0 \\ 0 & 0 & \sigma_{33} \end{bmatrix} \quad (1)$$

To consider the effects of molecular motion the shielding tensor is transformed to the axis system of molecular motion by use of an Euler transformation matrix \underline{R} . The orientation of the new frame with respect to a previous one is defined by a set of Euler angles, $\Omega = \alpha, \beta, \gamma$. If a positive rotation is to be applied to a frame (x,y,z) about the Euler angles (α, β, γ), then

$$\underline{R}(\alpha\beta\gamma) = \underline{R}_{zz}(\gamma)\underline{R}_{yy}(\beta)\underline{R}_{zz}(\alpha) \quad (2)$$

where α is a rotation about the original z axis, β is about the new y axis, and γ is about the final z axis. The product of the three rotation matrices leads to

$$\underline{R}(\alpha\beta\gamma) = \begin{bmatrix} \cos\alpha\cos\beta\cos\gamma & \sin\alpha\cos\beta\cos\gamma & -\sin\beta\cos\gamma \\ -\sin\alpha\sin\gamma & +\cos\alpha\sin\gamma & \\ -\cos\alpha\cos\beta\sin\gamma & -\sin\alpha\cos\beta\sin\gamma & \sin\beta\sin\gamma \\ -\sin\alpha\cos\gamma & +\cos\alpha\cos\gamma & \\ \cos\alpha\sin\beta & \sin\alpha\sin\beta & \cos\beta \end{bmatrix} \quad (3)$$

benzene,²² is oriented with the σ_{11} axis parallel to the C-H bond and the σ_{33} axis perpendicular to the ring plane. The σ_{22} axis is in the ring plane, perpendicular to the C-H bond. In the previous communication,¹⁴ the principal values of the shielding tensor were calculated by matching theoretical spectra generated on the basis of the Bloembergen-Rowland equations²³ with the experimental spectra at -160°C . A reasonably good fit between calculated and observed spectra is found by using $\sigma_{11}=17\pm 1$, $\sigma_{22}=52\pm 1$, and $\sigma_{33}=175\pm 1$ ppm on the CS_2 scale and a Lorentzian line broadening of 320 Hz. In simulating σ_{11} , σ_{22} , and σ_{33} , we assume that the frequency of all molecular reorientations is small compared to $(\sigma_{11}-\sigma_{33})$ at -160°C . This is a good assumption as even at -140°C and -120°C the spectra can be simulated with these values; and thus we have met the "rigid lattice" condition. These principal values correspond to an isotropic chemical shift of 70 ± 3 ppm, which compares well with the observed chemical shift in solution of 72.5 ppm.

With the onset of motion, the chemical shift tensor will be averaged depending on the character of the geometry and rate of reorientation. If the nucleus under examination was undergoing fast, random reorientation then the chemical shift tensor would be reduced to just its isotropic value, as is evident for a rapidly tumbling molecule in solution. For a restricted reorientation or a slowly reorienting molecule, only a part of the chemical shift dispersion will be averaged out and the spectrum will change accordingly. Having defined the principal values of the shielding tensor and possessing knowledge of their orientation in the molecular frame, possible motions for the phenylene group were modeled in an attempt to simulate the highest temperature spectra at $+120^\circ\text{C}$. The line shape at this temperature is narrower and closer to an axially symmetric line shape when compared to the

All NMR measurements were made with a Bruker SXP 20-100 spectrometer. Temperature control was maintained to within $\pm 2\text{K}$ with a Bruker B-ST 100/700 temperature controller.

RESULTS

The temperature dependence of the changing CSA line shape is shown in Figure 1.

For the proton spin-lattice relaxation data at 90 MHz, the decay of the magnetization at all temperatures follows a simple exponential dependence with delay time, τ . The spin-lattice relaxation time, T_1 , is easily calculated from a linear least squares analysis of $\ln(A_\infty - A_\tau)$ vs. τ , where the A's are signal amplitudes and τ is the delay time. The uncertainty in a given T_1 value is $\pm 10\%$.

The proton $T_{1\rho}$ data is characterized from a linear least squares analysis of $\ln A$ vs. τ , where A is still the signal amplitude but τ is now the length of the locking pulse. The deviations from simple exponential decay are small and not indicative of a dispersion of relaxation times so a fit of the whole curve to a single exponential decay is employed. Similar behavior was previously reported for the proton $T_{1\rho}$ decay curves of the chloral polycarbonate. The error in a given $T_{1\rho}$ value is $\pm 15\%$ and both T_1 and $T_{1\rho}$ data are summarized as a function of temperature in Figure 2.

INTERPRETATION

CSA Tensor Line Shapes

The carbon-13 labelled polycarbonate allows one to study the chemical shift anisotropy line shape of this phenylene carbon. The principal axis system for the chemical shift tensor of aromatic carbons, as reported for

EXPERIMENTAL

The polycarbonate of bisphenol-A, single site carbon-13 enriched (>90%) on one of the two phenylene carbons ortho to the carbonate was synthesized from enriched phenol (2-carbon-13) obtained from KOR Isotopes, Inc. The methyl deuterated analogue of the bisphenol-A polycarbonate was obtained from standard synthetic techniques.²¹ The methyl groups were found to be 97% deuterated as determined from proton and deuterium spectra of the dissolved polymer.

The carbon CSA spectra were obtained for a dried powdered sample using cross polarization followed by high power proton decoupling at a carbon frequency of 22.636 MHz and a proton frequency of 89.995 MHz. Rotating fields of about 1.0 mT for protons and 4.0 mT for carbon were used with a contact time of 3 ms. Several hundred free induction decays were averaged at each temperature before Fourier transformation to give the absorption spectra. Line shapes recorded without cross polarization were found to be experimentally indistinguishable. To obtain a standard reference for the line shapes at each temperature, the first moment was numerically calculated for each spectrum and assigned the value of 72.5 ppm on the CS₂ scale, which is the isotropic shift found for this phenylene carbon in solution.

Proton spin-lattice relaxation times for a dried powdered samples of BPA-d₆ were measured at the Larmor frequency of 90 MHz. The $\pi/2$ pulse width was 2 μ s; and a standard π - τ - $\pi/2$ pulse sequence was used with a cycle time greater than 5 times T_1 . Proton spin-lattice relaxation times in the rotating frame were measured at a radio frequency field strength of 1.0 mT using a standard $\pi/2$ -phase shifted locking pulse sequence.

30-40° about the same axis. In this report, the previous CSA line shape analysis for a sample of carbon-13 labelled BPA, where 90% of one of the two phenylene carbons ortho to the carbonate are isotopically enriched, is extended over the temperature range of -160°C to +120°C in an attempt to characterize the rate and amplitude of the phenylene group motion as a function of temperature.

On its own, such a study suffers from the limited frequency dependence of the changing chemical shift anisotropy dispersion. To circumvent this problem, proton spin-lattice relaxation times, T_1 's, at the Larmor frequency of 90 MHz and spin-lattice relaxation times in the rotating frame, $T_{1\rho}$'s, are measured for a methyl deuterated analogue of BPA (BPA- d_6) so that a more thorough analysis of the time scales and energetics of the phenylene motion may be obtained. These latter studies parallel an earlier proton analysis of the chloral polycarbonate¹⁴ in which a quantitative interpretation of the phenylene proton relaxation data was offered based on a homogeneous correlation function¹⁶ for motional modulation of the dipole-dipole interaction. The greatest interpretational success was obtained by using a fractional exponential correlation function which has been developed on the basis of correlated state excitations in condensed matter by Ngai¹⁷⁻¹⁹ and empirically by Williams and Watts.²⁰ As with the chloral polycarbonate, if the NMR relaxation data for BPA- d_6 can be successfully quantified with the correlation function, then the temperature dependent spectral densities obtained from the spin relaxation studies can be used to predict the temperature and frequency of the dynamic mechanical response.

INTRODUCTION

Over the past few decades there has been considerable interest in using NMR to define and quantify the motional processes which occur in bulk polymers below the glass transition temperature, T_g .^{1,2} At temperatures greater than T_g , a polymer chain may undertake a wide variety of motions; however below T_g many of these become modified, in particular the long-range motions. Polymers frequently reveal secondary transitions which are thought to arise from specific types of local motion still present in the glass.

One group of polymers in particular, the polycarbonate of bisphenol-A (BPA) and its structurally related analogues, has received much attention. This intense interest is fueled by the fact that BPA exhibits good impact resistance over a temperature range more than 250°C below the glass transition temperature ($T_g \sim 145^\circ\text{C}$).³ Dynamic mechanical and dielectric spectroscopy studies at 1 Hz reveal that BPA has an especially prominent secondary transition peak at approximately -100°C .⁴⁻⁷ It can be noted that nearly all glassy polymers which exhibit high impact strength have prominent secondary transitions, thus arguing for some relationship between the bulk mechanical properties and the extensive, rapid motion in the glass.⁸

Recently there has been significant structural and dynamical information developed on the polycarbonates from NMR.⁹⁻¹² In particular, the geometry of the phenylene group reorientation in BPA in the limit of rapid motion in the bulk below T_g has been characterized through the use of deuterium,¹³ chemical shift anisotropy (CSA),¹⁴ and dipolar rotational spin-echo carbon-13 line shapes.¹⁵ The basic conclusion reached by all is that the principal motion of the phenylene groups may be characterized as π flips about the C_1C_4 axis in combination with a small restricted angular oscillation of approximately

ABSTRACT

Carbon-13 chemical shift anisotropy (CSA) line shapes and proton relaxation data are used to establish the time scale and amplitudes of phenylene group motions in glassy polycarbonate as a function of temperature. The phenylene group undergoes both π flips and restricted rotation. The rate of π flips and the amplitude of restricted rotation are determined from simulating the carbon-13 CSA line shapes. Using a simple exponential correlation function, an activation energy of $11 \pm 5 \text{ kJ/mol}$ is found for the π flip rate. The root mean square angular amplitude varies linearly with temperature to the one-half power. The π flip rate is found to lie on the same line on a relaxation map as the proton relaxation minima, dielectric loss maxima and dynamic mechanical loss maxima. Analysis of the relaxation map gives an apparent activation energy of $48 \pm 5 \text{ kJ/mol}$. The discrepancy between the two activation energies arises from the limited frequency range and simple correlation function employed in the CSA analysis. A Williams-Watts-Ngai fractional exponential correlation function with Arrhenius parameters set from the relaxation map can account for the breadth and position of the proton relaxation minima and the dynamic mechanical loss peak.

The Temperature Dependence of Local Motions in Glassy Polycarbonate

From Carbon and Proton NMR

J. F. O'Gara, A. A. Jones* and C.-C. Hung

Jeppson Laboratory

Department of Chemistry

Clark University

Worcester, MA 01610

and

P. T. Inglefield

Department of Chemistry

College of the Holy Cross

Worcester, MA 01610

the interpretation of the proton and carbon-13 relaxation times in polyacarbonates.

DISCUSSION AND CONCLUSIONS

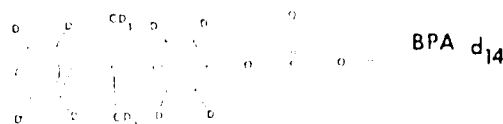
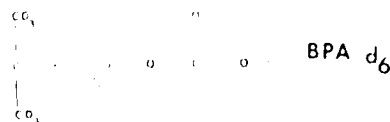
These results are in contrast to the observations previously developed from carbon-13 relaxation measurements. Since relaxation in this study employing a proton NMR, the effect of relaxation on the ability to obtain the T_1 is present in the proton and not in the carbon-13, the relaxation times are required. The relaxation times in the proton are of the order of 10^{-4} to 10^{-5} sec, which will allow the use of the proton NMR to provide a more accurate measurement of the relaxation times of the carbon-13. The relaxation times of the carbon-13 are of the order of 10^{-2} to 10^{-3} sec, which will allow the use of the carbon-13 NMR to provide a more accurate measurement of the relaxation times of the proton. The relaxation times of the proton are of the order of 10^{-4} to 10^{-5} sec, which will allow the use of the proton NMR to provide a more accurate measurement of the relaxation times of the carbon-13. The relaxation times of the carbon-13 are of the order of 10^{-2} to 10^{-3} sec, which will allow the use of the carbon-13 NMR to provide a more accurate measurement of the relaxation times of the proton.

Acknowledgments

This research was supported by the National Science Foundation Grant No. 1577, Army Research Office (Durham) Grant No. 1577, and the National Science Foundation Grant No. 1577. The authors are grateful to the National Science Foundation for its support of this research.

References

- (1) Jones, A.A., *Macromolecules*, **12**, 1136.
- (2) Ottewill, F.S., *Macromolecules*, **12**, 1136.
- (3) Ottewill, F.S., *Macromolecules*, **12**, 1136.
- (4) Hall, G.K., *Macromolecules*, **12**, 1136.
- (5) Natta, G., *Macromolecules*, **12**, 1136.
- (6) Janz, A.L., *Macromolecules*, **12**, 1136.
- (7) Abramson, A., *Macromolecules*, **12**, 1136.
- (8) Miller, E.V., *Macromolecules*, **12**, 1136.
- (9) Hertz, H., *Macromolecules*, **12**, 1136.
- (10) Schrieffer, J.R., *Macromolecules*, **12**, 1136.
- (11) Mott, N.F., *Macromolecules*, **12**, 1136.
- (12) Hohenberg, G.E., *Macromolecules*, **12**, 1136.
- (13) Lurie, M.E., *Macromolecules*, **12**, 1136.



Received May 1, 1967

square displacement versus the square root of temperature which provides a summarization of the temperature dependence of the oscillation.

Relaxation Data

The limited frequency range of the changing CSA dispersion does not warrant a more complex interpretation of the time dependence of the phenylene group motion by itself. As mentioned in the Introduction, proton spin-lattice relaxation measurements carried out in both the Zeeman frame and the rotating frame will be used to characterize the rate dependence of the phenylene motion in a similar manner as was done for the chloral polycarbonate.¹¹ Both T_1 and $T_{1\rho}$ can be quantitatively simulated as a function of temperature with a given correlation function and the associated spectral density. The standard T_1 and $T_{1\rho}$ expressions are used¹¹

$$\begin{aligned} 1/T_1 &= (2/3)\gamma^2 S [J_1(\omega_H) + 4J_2(2\omega_H)] \\ 1/T_{1\rho} &= (2/3)\gamma^2 S [1.5J_e(2\omega_e) + 2.5J_1(\omega_H) + J_2(2\omega_H)] \end{aligned} \quad (14)$$

where $\omega_e = \gamma_H H_{rf}$ and S is the motionally modulated component of the second moment. The applicability of these equations and this approach has been presented for chloral polycarbonate and the current situation is quite similar.

Given the previous success of the fractional exponential correlation function in modeling the relaxation behavior of the chloral polycarbonate, it is again chosen to simulate the BPA- d_6 data. The correlation function can be expressed in the Ngai formalism¹⁷⁻¹⁹ as

$$\phi(t) = \phi(0) \exp[-(t/\tau_p)^{1-n}] \quad (15)$$

where $0 < n < 1$ and

$$\tau_p = [(1-n) \exp(n\gamma) E_c^n \tau_0]^{1/(1-n)} \quad (16)$$

where $\tau_0 = \tau_\infty \exp(E_A/RT)$, the microscopic correlation time, E_C the bath cutoff energy and $\gamma = 1.577$ Euler's constant. The parameters τ_∞ and E_A fix the microscopic dynamics and energetics of the fundamental process in the absence of correlated state coupling. The parameters n and E_C determine the width of the frequency dispersion and the renormalized time scale due to medium effects. For $n \neq 0$, $\tau_p = \tau_\infty^* \exp(E_A^*/RT)$ where E_A^* is the apparent activation energy, given by $E_A^* = E_A/(1-n)$ and the apparent preexponential is given by

$$\tau_\infty^* = [(1-n) \exp(n\gamma) E_C^n \tau_\infty]^{1/(1-n)}.$$

The actual parameters varied to fit experimental data are E_A^* , τ_∞^* and n . In order to get a handle on the values of E_A^* and τ_∞^* for the BPA- d_6 relaxation data, a relaxation map, $\log \nu_C$ vs. T^{-1} , was constructed. The temperature positions of T_1 and $T_{1\rho}$ minima each can be assigned an appropriate correlation frequency as outlined by McCall.¹ One can also associate a correlation frequency with the CSA line shape collapse. The average frequency difference between the two sites corresponding to the two positions of the phenylene group is $\delta\nu = 700$ Hz where the average is over all orientations. The correlation frequency in Hertz that corresponds to the collapse of this can be estimated²⁷ from $\nu_C = \frac{\delta\nu}{2\sqrt{2}}$ and the associated temperature can be obtained from the plot of π flip rate versus inverse temperature in Figure 4. Furthermore, one can also justify adding frequency points corresponding to the temperatures of the maxima in dynamic mechanical⁴ and dielectric relaxation²⁶⁻²⁸ data as found in the literature. First, the previous work with the chloral polycarbonate indicated a good correlation between the dynamic mechanical loss peak at low temperature and the phenylene proton NMR data. Second, it

has long been argued that an apparent coupling or cooperativity exists between phenylene group motion and motion involving the carbonate as evidenced by both dilute solution¹⁴ and solid state experiments.⁵⁻⁷ A plot of the $\log \nu_c$ vs. T^{-1} containing the various experimental results is presented in Figure 6. A linear least squares analysis of this data allows for a determination of $E_A^* = 48$ kJ/mol from the slope and $\tau_\infty^* = 1.06 \times 10^{-16}$ s from the intercept.

The $T_{1\rho}$ and T_1 data can then be simulated by simply varying n and S , given the E_A^* and τ_∞^* from the relaxation map. The best fit as shown in Fig. 2 was obtained with $n = .82$ and $S = 1.8 \times 10^{-2}$ mT². These values of the model parameters are physically reasonable. The activation energy of the fundamental process, E_A , (obtained from the Ngai formalism in the absence of correlated state coupling) which has been identified as π flips of the phenylene rings, is 8.6 kJ/mol; and can be compared to the dilute solution value of 13 kJ/mol for phenylene rotation obtained in an earlier solution study.³¹ The solution activation energy should be slightly higher than E_A since even in a 10 wt% solution the surroundings will affect the fundamental process. The magnitude of n indicates that in the bulk glass the phenylene motion is strongly affected by the medium. The apparent activation energy in the glass is substantially higher, 48 kJ/mol. The value of S , the proton second moment, used in equation 14 should correspond to the motionally modulated component of the second moment. This motionally modulated dipole-dipole interaction corresponds to part of the intermolecular dipole-dipole contributions since the predominant motion causing modulation is phenylene ring motion about the C_1C_4 axis which does not reorient the largest intramolecular dipole-dipole interaction. The second moment is not given an explicit temperature depen-

dence except through the spectral density as indicated by equation (14). A detailed proton line shape has not been carried out here but preliminary results indicate the second moment behavior parallels the earlier chloral polycarbonate study.¹⁰ The amount of motionally modulated second moment employed here is consistent with the experimental value of $1.5 \pm 0.4 \times 10^{-2} \text{ mT}^2$ observed at the highest temperature of that study.

To further probe the success of this molecular modeling, the position and shape of the dynamic mechanical loss peak located at about -100°C at 1 Hz, the gamma peak as measured by Yee,⁴ was analyzed. The mechanical loss $G_Y(\omega)^{\text{loss}}$, is given by the following equation

$$G_Y(\omega)^{\text{loss}} = \frac{\langle \sigma_Y(0)^2 \rangle}{k_B T} \int_0^\infty \sin(\omega t) \phi'(t) dt \quad (17)$$

where $\phi'(t)$ is the derivative of the correlation function. One sees in Figure 7 that much of the shape and temperature dependence is well simulated without further parameter adjustment of E_A^* , τ_∞^* , or n . The magnitude of the calculated loss peak is controlled by $\langle \sigma_Y(0) \rangle$ which is adjusted to match the data.

DISCUSSION

Carbon-13 chemical shift anisotropy line shape analysis serves to definitively characterize the geometry of phenylene group motion as a combination of π flips and restricted rotation. The π flip rate is found to lie on a relaxation map containing proton T_1 and $T_{1\rho}$ minima, dielectric loss maxima and dynamic mechanical loss maxima. This combination of such a broad sampling of frequency results in a more accurate time scale and activation energy analysis. A single exponential correlation function, as was used in the simple two site jump model for the temperature dependence of the CSA line shapes, is in-

adequate for the simulation of the T_1 , $T_{1\rho}$, and dynamic mechanical loss data. It follows that the activation energy from a single correlation time analysis may be in serious error.

This phenomenological link in time between the various relaxation experiments can be quantitatively summarized in terms of a fractional exponential correlation function. This function reasonably approximates the shape and position of the T_1 and $T_{1\rho}$ minima versus temperatures as well as the temperature position and breadth of the dynamic mechanical loss peak. Such a connection between the relaxation experiments argue for a common underlying dynamic process which produces NMR, dielectric and mechanical relaxation.

There are, however, some questions raised by this conclusion. Jumps of the phenylene group between symmetric minima are unlikely to produce a large mechanical loss¹⁶ and certainly will not produce a dielectric loss. A recent proposal³² suggests that the common motion leading to the several relaxation effects is a correlated interchange³³ of carbonate group conformations. A cis-trans carbonate conformation is interchanged with a trans-trans carbonate conformation by rotations about backbone CO bonds. This motion reorients carbonate groups which could lead to dielectric and shear loss. The BPA unit between the two carbonates interchanging conformations is translated but not significantly reoriented. The π flips are tied to this correlated backbone motion by intramolecular and intermolecular interactions which places the π flips on a relaxation map in common with dielectric and dynamic mechanical loss peaks. While this proposed motion cannot be completely verified; it is however, consistent with the observed relaxation phenomena.

The fractional exponential used to summarize the relaxation phenomena is cast in the Ngai form and yields realistic values for the apparent activated energy E_A^* and the microscopic activation energy E_A . This aspect assumes the fractional exponential correlation function is homogeneous though this is not required to simulate the relaxation minima and loss maxima. Dilute solution studies yield comparable values of E_A for both phenylene group rotation and correlated segmental motion which also appear to be linked in the dissolved polymer.¹⁴ Comparably low values for rotational barriers in BPA polycarbonate have been noted in theoretical calculations.³⁴⁻³⁵ These generally low barriers may be the key to the presence of such extensive dynamic freedom in the glass as has been proposed by Tonelli³⁴ though only solid state NMR line shape data has provided the basis to discriminate between various possible motions. Since virtually all intramolecular rotational barriers are low in polycarbonate and yet only certain reorientations are observed, intermolecular interactions must determine the nature of the motion in the glass. It is known that the BPA unit does not reorient except for π flips and restricted oscillation and this can be attributed to the difficulty of rotating such a large group in the glass. The proposed conformational interchange does not reorient the BPA unit though the smaller carbonate unit is reoriented. Again a conformational interchange is proposed so long range chain end rotation or translation is not required. A carbon-13 CSA line shape study has also been carried out on the carbonate unit.³⁶ Little line shape change is noted here which is difficult to reconcile with the presence of a large dielectric loss peak. However, the proposed conformational interchange involves a polycarbonate chain where most units are trans-trans and a smaller number of units are

cis-trans. Thus the carbonate unit would predominantly reflect the trans-trans CSA tensor and orientation. However, the conformational interchange leads to diffusion of the cis-trans conformation so all units can undergo re-orientation though the time scale is complex.

The temperature dependence of the oscillation of the phenylene group about the C_1C_4 axis is also interesting. The rms amplitude is apparently linear versus temperature to the one-half power which is to be expected for a harmonic potential. However, the amplitude also ought to go to zero at a temperature of absolute zero for a harmonic potential. The simulation does not yield this result and the significance of the behavior shown in Figure 5 will be the subject of a subsequent paper.

ACKNOWLEDGEMENT

This research was carried out with the financial support of the National Science Foundation Grant DMR-790677, of National Science Foundation Equipment Grant No. CHE77-09059, of National Science Foundation Grant No. DMR-8108679 and of U.S. Army Research Office Grant DAAG 29-82-G-0001.

REFERENCES

1. McCall, D. W., Accounts Chem. 4 , 223.
2. McBrierty, V. J.; Douglass, D. C., Physics Reports 1980, 63 (2), 61.
3. Heijboer, J., J. Polym. Sci., Part C 1966, 16, 3755.
4. Yee, A. F.; Smith, S. A., Macromolecules 1981, 14, 54.
5. Matsuoka, S.; Ishida, Y., J. Polym. Sci., Part C 1966, 14, 247.
6. Massa, D. J.; Flick, J. R., Polym. Prepr., Am. Chem. Soc., Div. Polym. Chem. 1973, 14 (2), 1249.
7. Massa, D. J.; Rusanowsky, R. P., Polym. Prepr., Am. Chem. Soc., Div. Polym. Chem. 1976, 17 (2), 184.
8. Nielsen, L. E., "Mechanical Properties of Polymers and Composites"; Marcel Dekker, Inc., New York, NY, 1974.
9. Schaefer, J.; Stejskal, E. O.; Buchdahl, R., Macromolecules 1977, 10, 384.
10. Inglefield, P. T.; Jones, A. A.; Lubianez, R. P.; O'Gara, J. F., Macromolecules 1981, 14 288.
11. Jones, A. A.; O'Gara, J. F.; Inglefield, P. T.; Bendler, J. T.; Yee, A. F.; Ngai, K. L., Macromolecules 1983, 16, 685.
12. Inglefield, P. T.; Amici, R. M.; O'Gara, J. F.; Hung, C.-C.; Jones, A. A., Macromolecules 1983, 16, 1552.
13. Spiess, H. W., Colloid Polym. Sci. 1983, 261, 193.
14. Connolly, J. J.; Gordon, E.; Jones, A. A., Macromolecules 1984, 17, 722.
15. Schaefer, J.; Stejskal, E. O.; McKay, R. A.; Dixon, W. T. Macromolecules 1984, 17 1479.
16. Garroway, A.N.; Ritchey, W.M.; Moniz, W.B. Macromolecules 1982, 15, 1051.
17. Ngai, K. L., Comments Solid State Phys. 1979, 9, 127.
18. Ngai, K. L.; White, C. T., Phys. Rev. B. 1979, 20, 2475.
19. Ngai, K. L., Phys. Rev. B. 1980, 22, 2066.
20. Williams, G.; Watts, D. C., Trans. Faraday Soc. 1970, 66, 80.

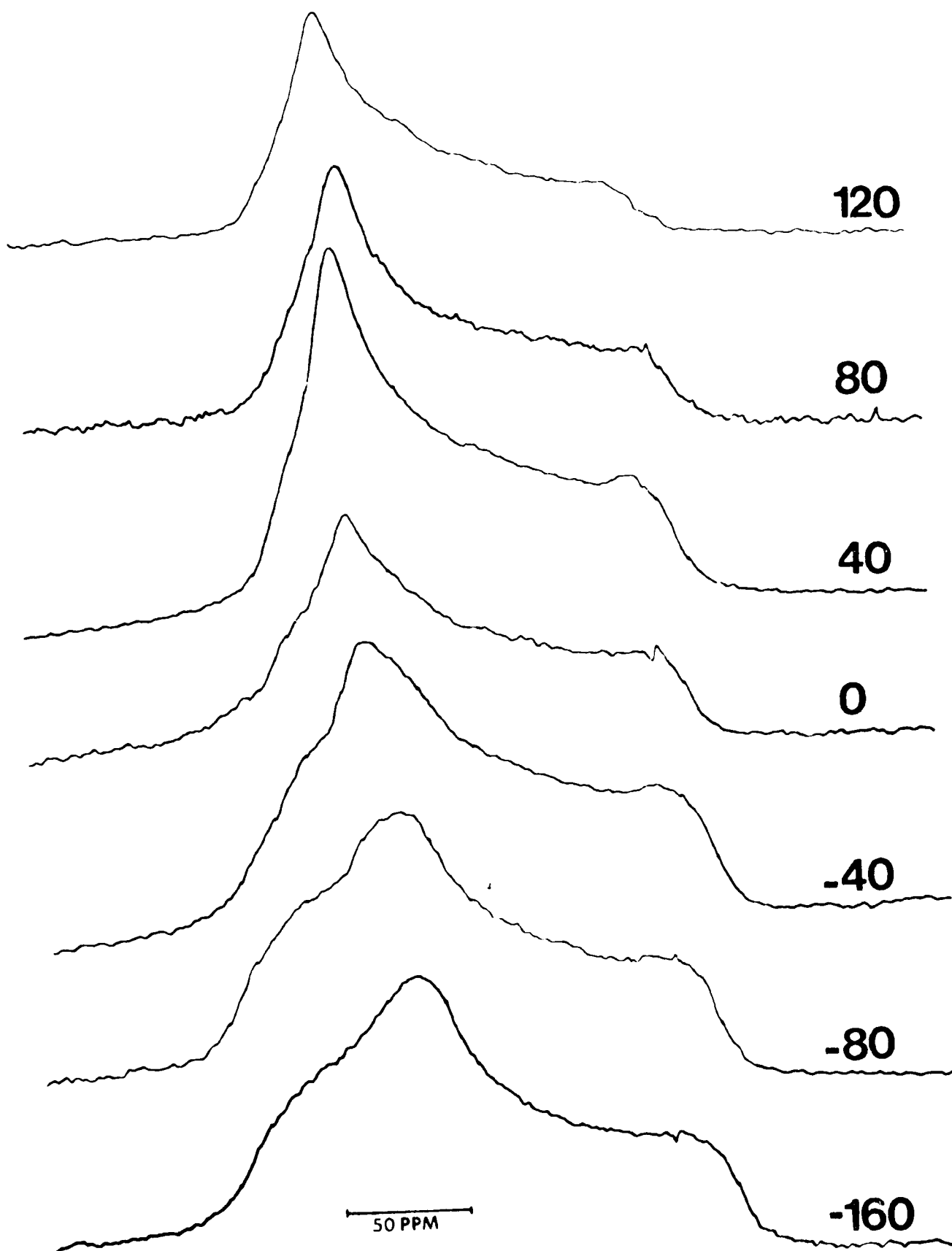
21. Schnell, H.; Krimm, A. *Agnew Chem. Internat. Edit* (1963) 2 No. 7.
22. Mehring, M., *NMR Basic Principles and Progress* 1976, 11.
23. Bloembergen N.; Rowland, T.J. *Acta. Metallurgica* 1955 1, 731.
24. Slotfeldt-Ellingsen, D.; Resing, H.A. *J. Phys. Chem.* 1980 84, 2204.
25. Wemmer, D.E. Ph.D. Thesis, University of California, Berkeley, CA, 1979.
26. Wemmer, D. E.; Ruben, D. J.; Pines, A., *J. Am. Chem. Soc.* 1981, 103, 28.
27. Sanstrom, J., "Dynamic NMR Spectroscopy"; Academic Press, New York, NY, 1982.
28. Illers, K. H.; Breur, H. *Kolloid-Z.* 1961, 176, 110.
29. Krum, F.; Miller, F. H., *Kolloid-Z.* 1959, 1959, 164.
30. Michailov, G. P.; Eidelnant, M. P., *Vysokomolekul. Soedin.* 1960, 2, 281.
31. Jones, A.A.; Bisceglia, M. *Macromolecules.* 1979 12, 136.
32. Jones, A.A. To appear in *Macromolecules*.
33. Hall, C. K.; Helfand, E. *J. Chem. Phys.* 1982, 77, 3275.
34. Tonelli, A.E. *Macromolecules* (1972) 5, 558.
35. Bendler, J. T., *New York Acad. Sci.* 1973, 6, 503. Bendler, J.T. *Ann. N.Y. Acad. Sci.* (1981) 371, 299.
36. Henrichs, P.M. To appear in *Macromolecules*.

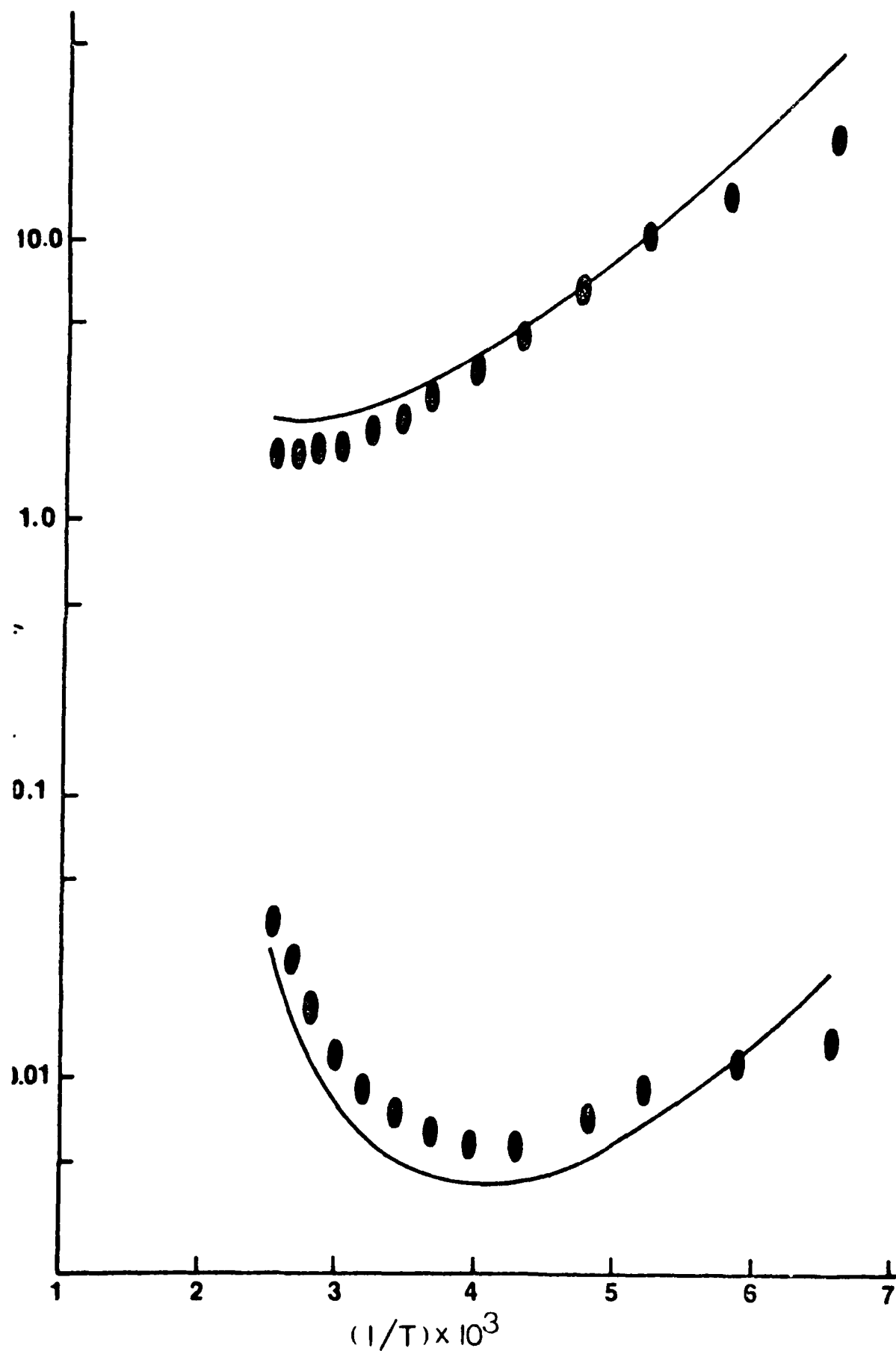
FIGURE CAPTIONS

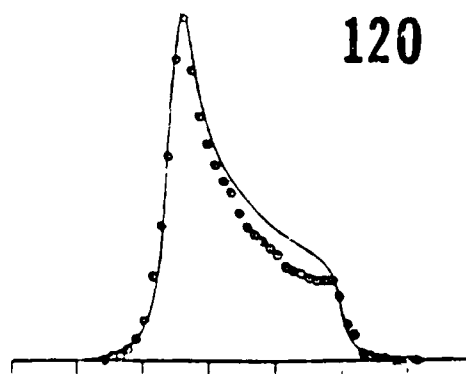
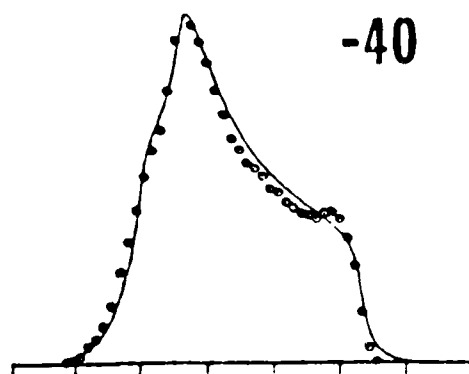
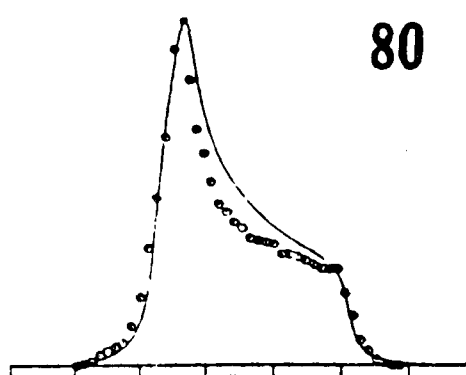
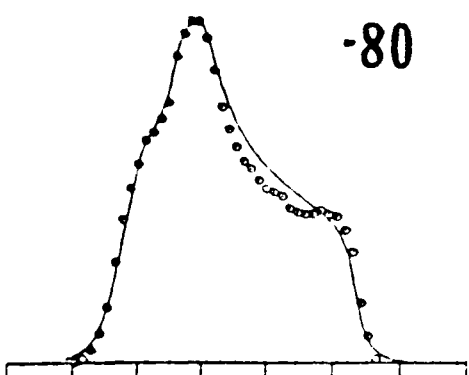
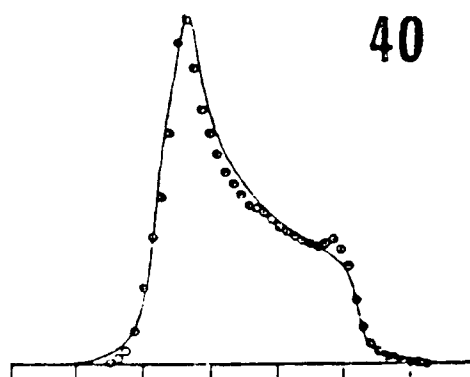
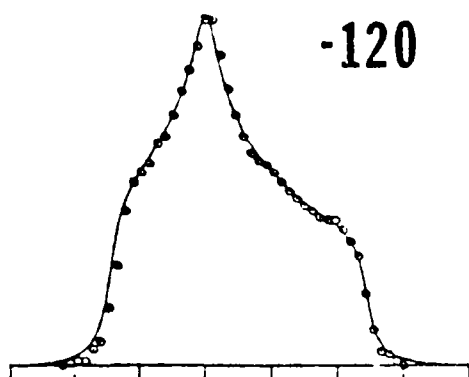
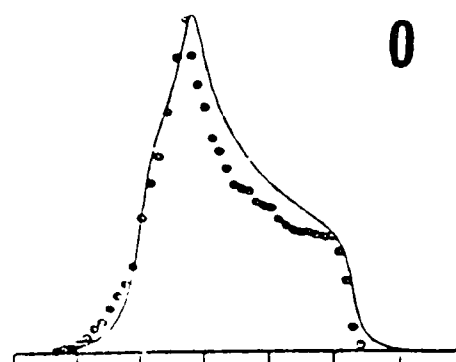
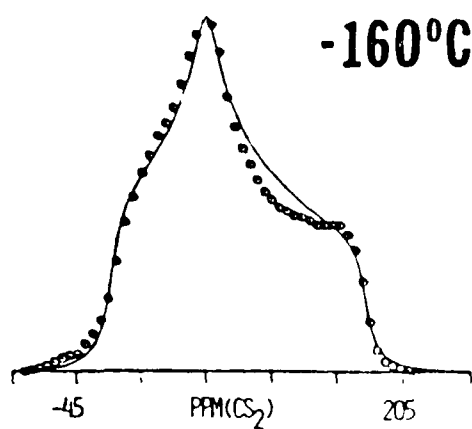
- Figure 1: Carbon-13 CSA line shapes at several temperatures.
- Figure 2: Proton spin-lattice relaxation times and proton spin-lattice relaxation times in the rotating frame versus inverse temperature. The solid line corresponds to a fit of the relaxation data with a Williams-Watts-Ngai fractional exponential correlation function.
- Figure 3: The lines are simulations of the carbon-13 CSA line shapes at several temperatures while the points are line shape data taken from Figure 1.
- Figure 4: The logarithm of the flip rate versus inverse temperature. The flip rate is determined from simulation of the carbon-13 CSA line shape.
- Figure 5: Root mean square amplitude of restricted phenylene group rotation about the C₁C₄ axis versus temperature to the one-half power. The rms amplitude is determined from simulating the carbon-13 CSA line shapes. The open circles are determined at temperatures where the oscillation is the primary source of narrowing and x's are estimates made at temperatures where the flips are the primary source of narrowing.
- Figure 6: Log frequency versus inverse temperature or relaxation map. The highest frequency NMR point is the 90MHz proton T₁ minimum. The next highest frequency NMR point is the 43kHz T₁ minimum. The lowest frequency NMR point is the position of maximum collapse of the carbon-13 chemical shift anisotropy line shape. The open circles are maxima of dielectric loss curves taken at different frequen-

cies. The positions of all points have an uncertainty of the order of 10 degrees because of the breadth of the loss peaks and relaxation minima.

Figure 7: Dynamic mechanical spectrum. The dashed line is the simulation employing the Williams-Watts-Ngai fractional exponential with the parameters set from the relaxation map.





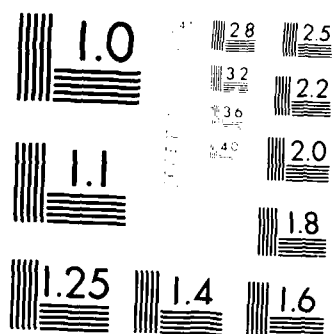


AD-A152 011 CHAIN DYNAMICS AND STRUCTURE PROPERTY RELATION IN HIGH 2/2
IMPACT STRENGTH PO. (U) COLLEGE OF THE HOLY CROSS
WORCESTER MA P T INGLEFIELD ET AL. 04 JAN 85
UNCLASSIFIED ARO-18501.7-CH-H DRAG29-82-G-0001 F/G 11/9 NL

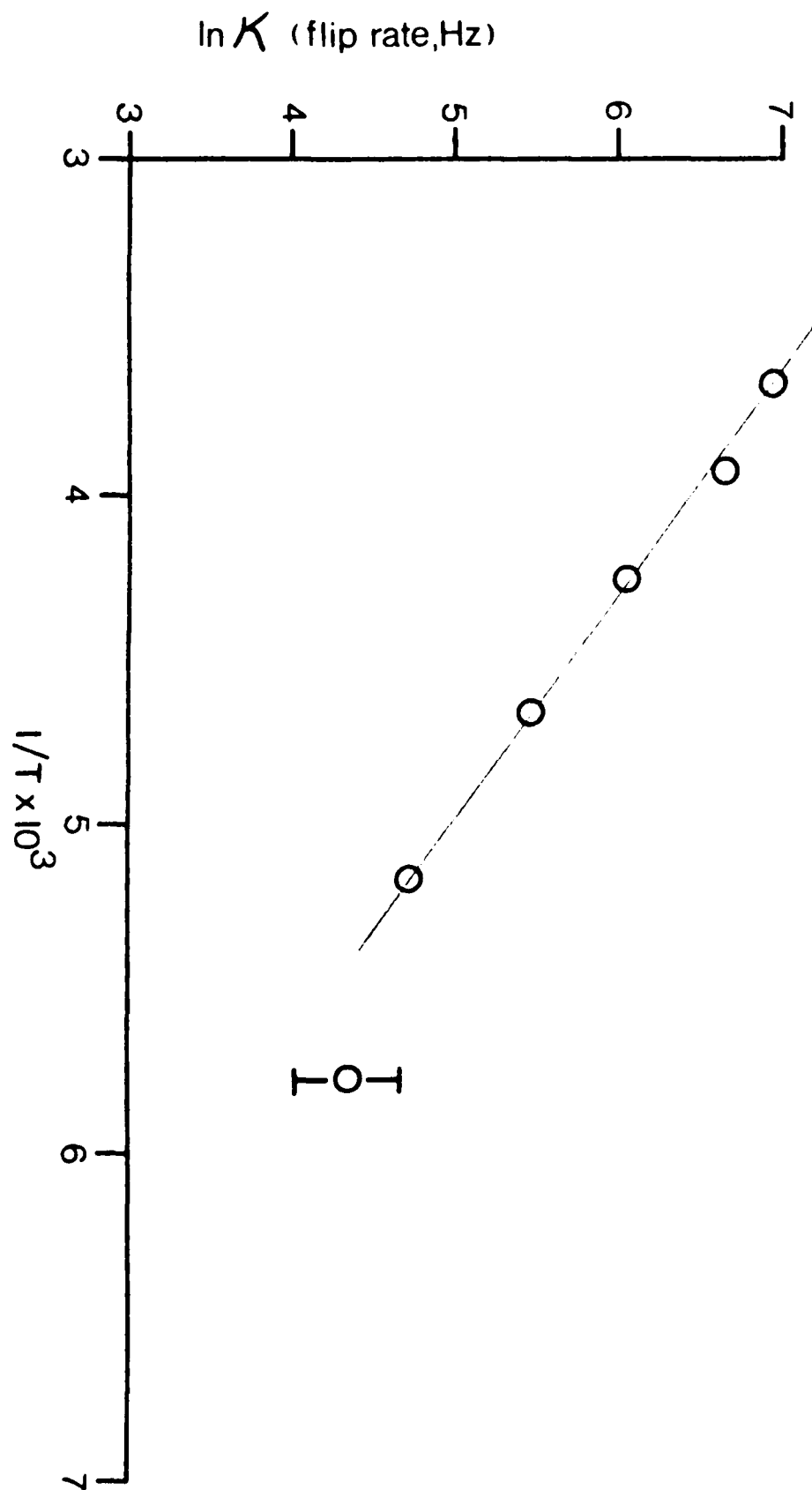
END

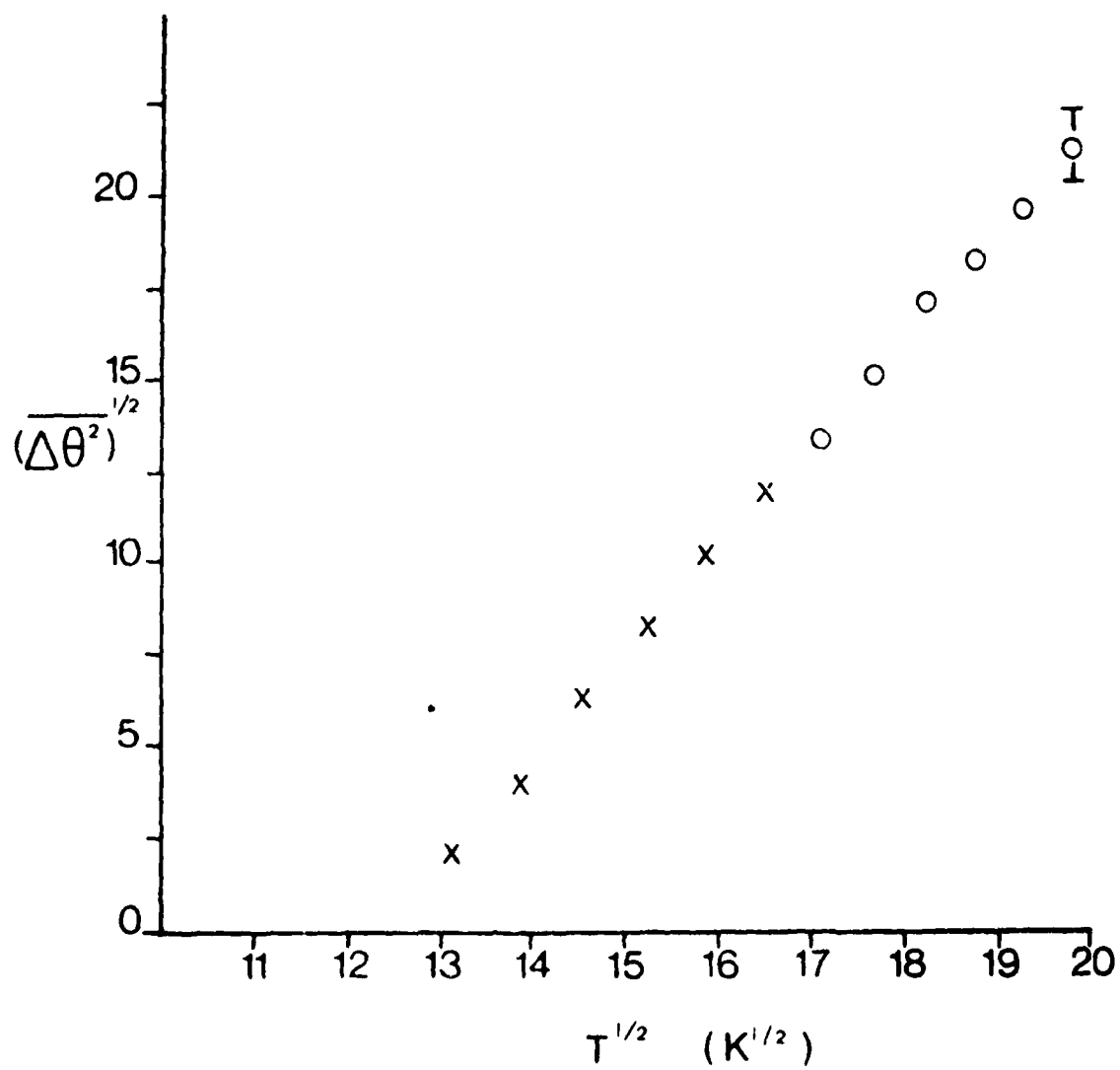
FORM

DATA

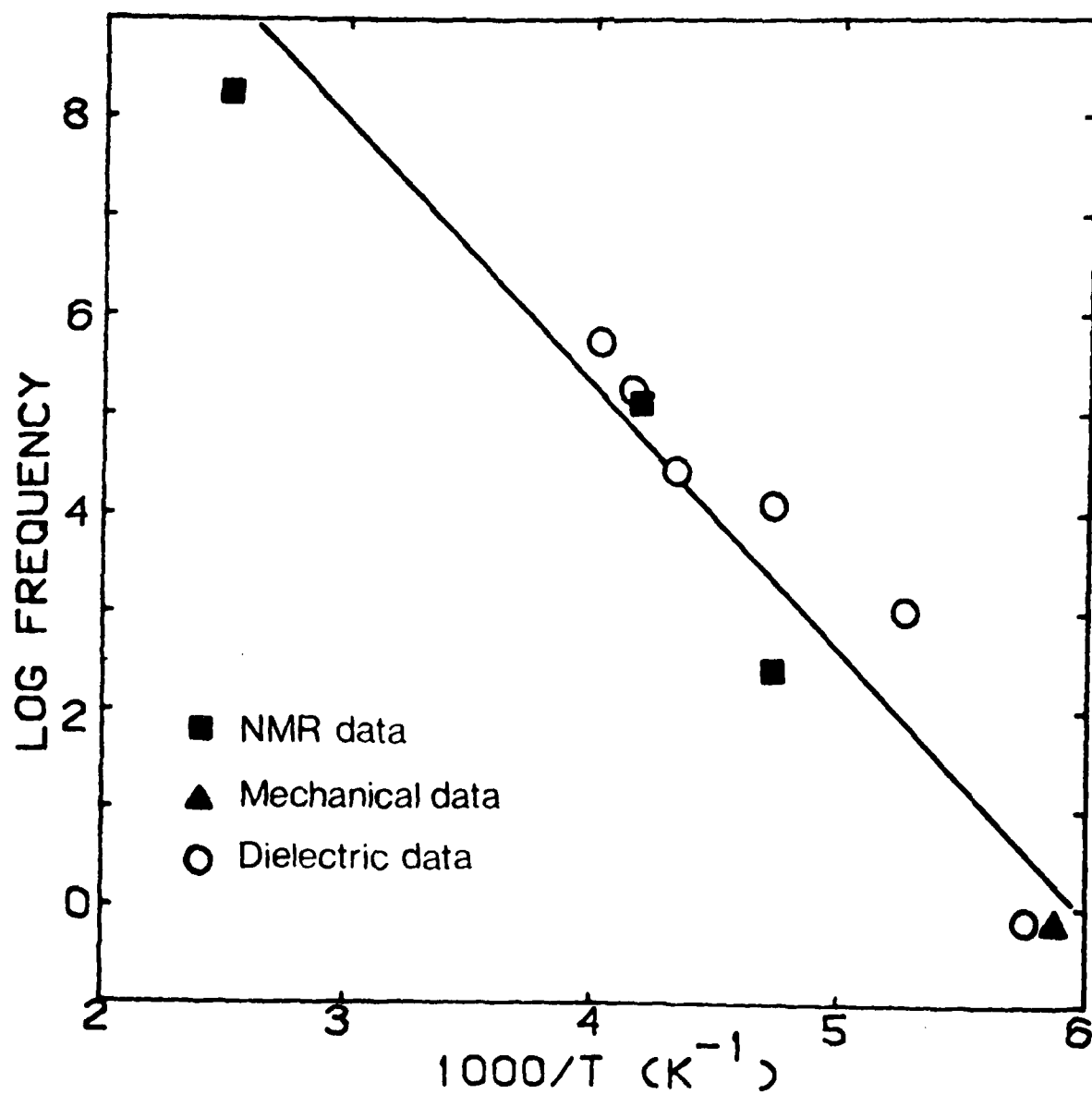


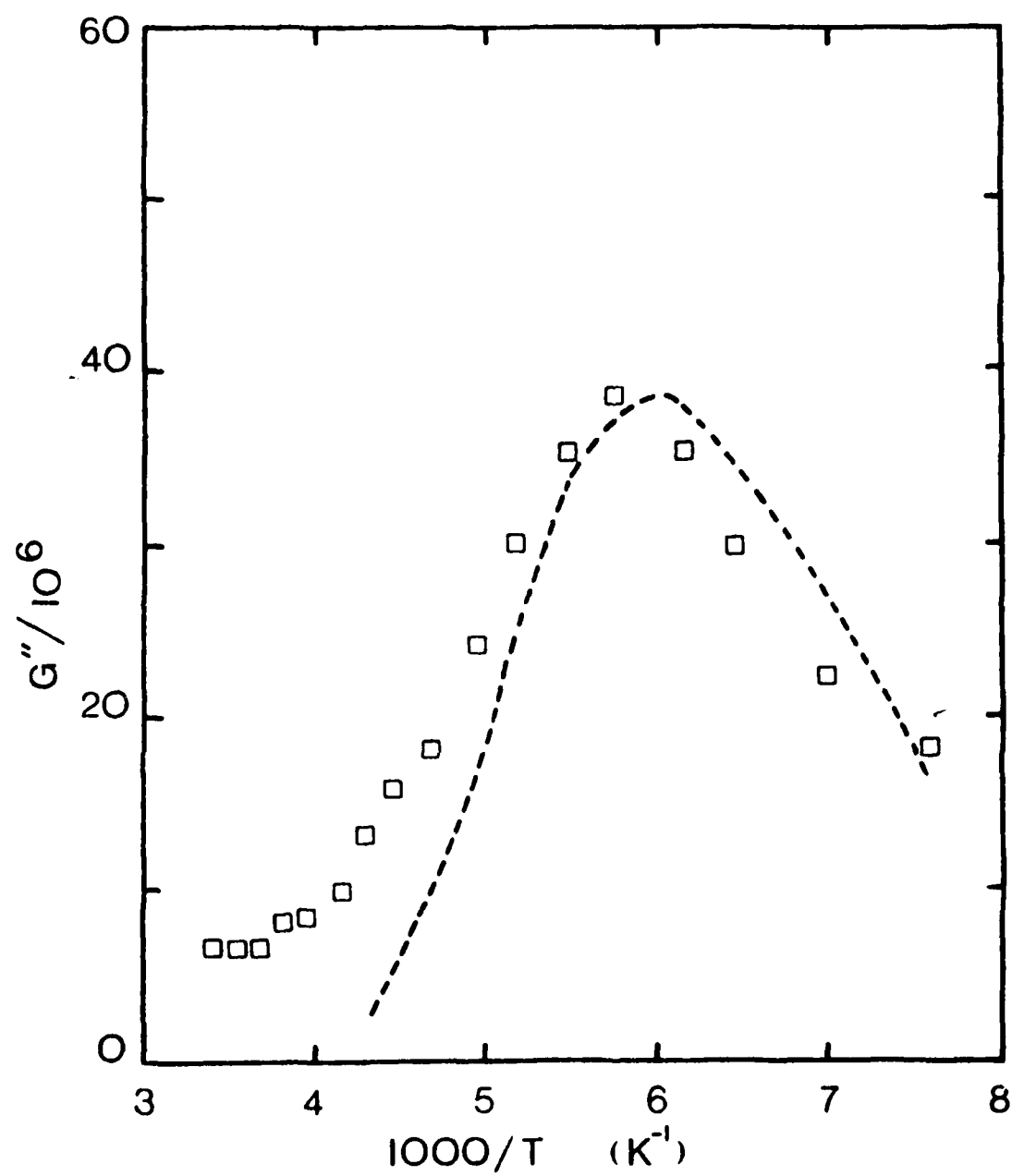
MICROCOPY RESOLUTION TEST CHART
 NATIONAL BUREAU OF STANDARDS-1963-A





RELAXATION MAP





END

FILMED

5-85

DTIC